Precambrian Research 198–199 (2012) 51–76

Contents lists available at SciVerse ScienceDirect

Precambrian Research

journal homepage: www.elsevier.com/locate/precamres

Paleomagnetic and geochronological studies of the mafic dyke swarms of Bundelkhand craton, central India: Implications for the tectonic evolution and paleogeographic reconstructions

Vimal R. Pradhan[a,*], Joseph G. Meert[a], Manoj K. Pandit[b], George Kamenov[a], Md. Erfan Ali Mondal[c]

[a] Department of Geological Sciences, University of Florida, 241 Williamson Hall, Gainesville, FL 32611, USA
[b] Department of Geology, University of Rajasthan, Jaipur 302004, Rajasthan, India
[c] Department of Geology, Aligarh Muslim University, Aligarh 202002, India

ARTICLE INFO

Article history:
Received 12 July 2011
Received in revised form 6 November 2011
Accepted 18 November 2011
Available online 28 November 2011

Keywords:
Bundelkhand craton, Mafic dykes, Central India, Paleomagnetism, Geochronology, Paleogeography

ABSTRACT

The paleogeographic position of India within the Paleoproterozoic Columbia and Mesoproterozoic Rodinia supercontinents is shrouded in uncertainty due to the paucity of high quality paleomagnetic data with strong age control. New paleomagnetic and geochronological data from the Precambrian mafic dykes intruding granitoids and supracrustals of the Archean Bundelkhand craton (BC) in northern Peninsular India is significant in constraining the position of India at 2.0 and 1.1 Ga. The dykes are ubiquitous within the craton and have variable orientations (NW–SE, NE–SW, ENE–WSW and E–W). Three distinct episodes of dyke intrusion are inferred from the paleomagnetic analysis of these dykes. The older NW–SE trending dykes yield a mean paleomagnetic direction with a declination = 155.3° and an inclination = −7.8° (κ = 21; α_{95} = 9.6°). The overall paleomagnetic pole calculated from these 12 dykes falls at 58.5°N and 312.5°E (dp/dm = 6.6°/7.9°). The overall mean direction calculated from four ENE–WSW Mahoba dykes has a declination = 24.7° and inclination = −37.9° (κ = 36; α_{95} = 15.5°). The virtual geomagnetic pole (VGP) for these four dykes falls at 38.7°S and 49.5°E (dp/dm = 9.5°/16.3°). A third, and distinctly steeper, paleomagnetic direction was obtained from two of the NE–SW trending dykes with a declination = 189.3° and inclination = 64.5°. U–Pb geochronology generated in this study yields a U–Pb Concordia age of 1979 ± 8 Ma for the NW–SE trending dykes and a mean $^{207}Pb/^{206}Pb$ age of 1113 ± 7 Ma for the Mahoba suite of ENE–WSW trending dykes, confirming at least two dyke emplacement events within the BC. We present global paleogeographic maps for India at 1.1 and 2.0 Ga using these paleomagnetic poles. These new paleomagnetic results from the ~2.0 Ga NW–SE trending Bundelkhand dykes and the paleomagnetic data from the Bastar/Cuddapah suggest that the North and South Indian blocks of the Peninsular India were in close proximity by at least 2.5 Ga.

The paleomagnetic and geochronological data from the Mahoba dyke is significant in that it helps constrain the age of the Upper Vindhyan strata. The pole coincides in time and space with the Majhgawan kimberlite (1073 Ma) and the Bhander–Rewa poles from the Upper Vindhyan strata. The most parsimonious explanation for this coincidence is that the age of the Upper Vindhyan sedimentary sequence is >1000 Ma.

1. Introduction

The Indian subcontinent holds a key position when attempting to unravel the intricacies of Precambrian paleogeography, such as the Paleoproterozoic Columbia supercontinent (Rogers, 1996; Rogers and Santosh, 2002; Meert, 2002; Santosh et al., 2003; Zhao et al., 2004a,b), the Meso-Neoproterozoic Rodinia supercontinent (McMenamin and McMenamin, 1990; Meert and Torsvik, 2003; Meert and Powell, 2001; Li et al., 2008), and the Ediacaran–Cambrian Gondwana supercontinent (Meert, 2003; Meert and Van der Voo, 1996; Burke and Dewey, 1972; Pisarevsky et al., 2008). India offers target rocks that are both accessible and of appropriate age for conducting paleomagnetic and geochronological investigations (Meert, 2003; Powell and Pisarevsky, 2002; Meert and Powell, 2001; Pesonen et al., 2003). These target rocks include Precambrian mafic dykes and dyke swarms that intrude the Archean–Paleoproterozoic cratonic nuclei, as well as volcanic and sedimentary successions exposed in the Dharwar and Aravalli protocontinents of the Indian peninsular shield (Fig. 1).

The correlation of mafic dyke swarms in terms of their distribution, isotopic age, geochemistry and paleomagnetism is critical in order to fully evaluate Precambrian plate reconstructions and

* Corresponding author. Fax: +1 352 392 9294.
E-mail address: vimalroy@ufl.edu (V.R. Pradhan).

0301-9268/$ – see front matter © 2011 Elsevier B.V. All rights reserved.
doi:10.1016/j.precamres.2011.11.011

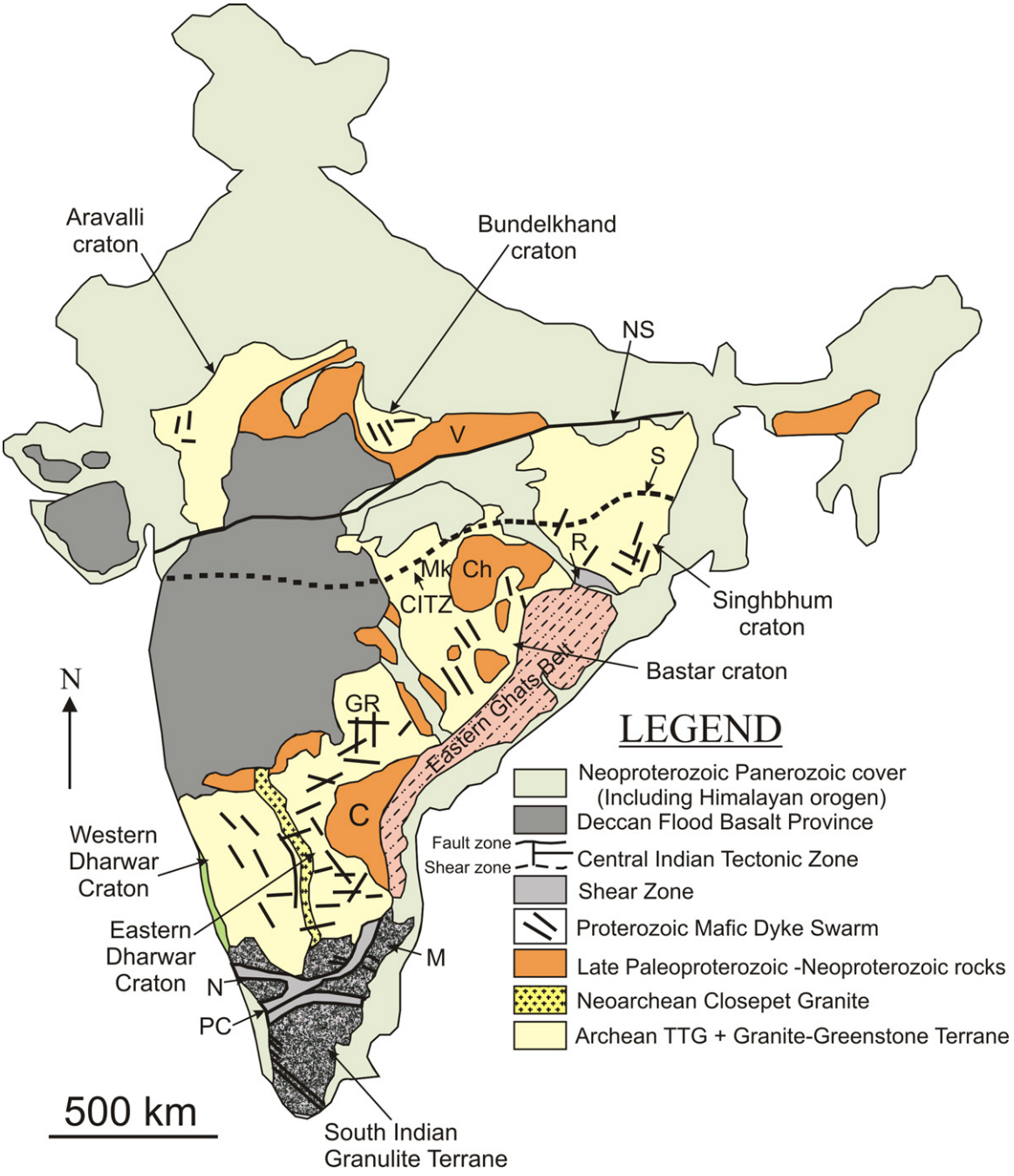

Fig. 1. Generalized geological and tectonic map of the Indian sub-continent with the Precambrian mafic dyke swarms cross-cutting various Archean cratonic blocks. C: Cuddapah basin; Ch: Chattisgarth Basin; CIS: Central Indian Shear Zone; GR: Godavari Rift; M: Madras Block; Mk: Malanjkhand; MR: Mahanadi Rift; N: Nilgiri Block; NS: Narmada–Son Fault Zone; PC: Palghat–Cauvery Shear Zone; R: Rengali Province and Kerajang Shear Zone; S: Singhbhum Shear Zone; V: Vindhyan Basin.
Source: (modified after French et al., 2008).

possible configuration of supercontinents (Halls, 1987; Van der Voo and Meert, 1991; Halls and Zhang, 1995; Mertanen et al., 1996; Park et al., 1995; Bleeker and Ernst, 2006; Ernst and Srivastava, 2008; Piispa et al., 2011). The Indian peninsular shield is traversed by numerous Precambrian mafic dyke swarms (Drury, 1984; Murthy et al., 1987; Murthy, 1995; Ramchandra et al., 1995; French et al., 2008; French and Heaman, 2010; Meert et al., 2010; Pati, 1999; Pati et al., 2008; Pradhan et al., 2008; Ernst et al., 2008; Srivastava and Gautam, 2008; Srivastava et al., 2008). These dykes intrude the granite-greenstone terranes of the major Indian cratonic nuclei, namely Dharwar in the south, Bastar in the east central, Singhbhum in the east and the Aravalli and Bundelkhand in the north–west and the north (Halls, 1982; Fig. 1). The dykes are the focus of considerable scientific attention aimed at defining their geochemical and geophysical characteristics, geochronology, paleomagnetism and tectonic controls on their emplacement (Devaraju et al., 1995, Radhakrishna and Piper, 1999; Srivastava et al., 2008; Halls et al., 2007; French et al., 2008; French and Heaman, 2010; Pradhan et al., 2008, 2010; Pati, 1999; Pati et al., 2008; Piispa et al., 2011; Ratre et al., 2010; Ernst et al., 2008; Ernst and Bleeker, 2010;

Meert et al., 2011). Paleomagnetic and geochronological studies on these Precambrian mafic dyke swarms as well as the volcanic and sedimentary successions of the Gwalior, Cuddapah and Vindhyan basins, provide insight into India's changing paleogeographic position during the critical Paleo- to Mesoproterozoic interval and may, in some circumstances, allow for further age constraints to be placed on the poorly dated sedimentary basins of India (Pradhan et al., 2008, 2010; Gregory et al., 2006; Malone et al., 2008; Meert et al., 2010, 2011; French et al., 2008; French, 2007; Halls et al., 2007; Ratre et al., 2010; French and Heaman, 2010; Piispa et al., 2011).

This study focuses on the Precambrian mafic dyke swarms intruding the Bundelkhand craton in north-central India (Pati, 1999). The most prominent of the Paleo–Mesoproterozoic (2.5–1.0 Ga) magmatic events are represented by three mafic dyke swarms that intrude the Archean granitic-gneissic basement of the Bundelkhand craton. The dykes follow two major trends, suggesting at least two major pulses of magmatic emplacement within the craton. Based on field cross-cutting relationships, the ENE–WSW trending dykes are the youngest in the craton, and are represented by the "Great Dyke of Mahoba" (Fig. 3c and d). Previous paleomagnetic studies on these dykes were hindered by poor age constraints (Poitou et al., 2008). Existing isotopic ages allow an age bracket between 2150 and 1500 Ma for the older suite of mafic dykes (Rao, 2004; Rao et al., 2005; Basu, 1986; Sarkar et al., 1997; Sharma and Rahman, 1996).

We report new paleomagnetic and geochronological data on the Bundelkhand mafic dykes from the Mahoba, Banda, Khajurao and nearby areas of the Bundelkhand province in the central India (Fig. 2). This study offers the first robust age constraints on the paleomagnetic poles calculated from these mafic dykes. These data will ultimately aid in improving our models for the Precambrian tectonic evolution of the Indian cratons, clarify the role of India in the Columbia and Rodinia supercontinents, and generate data for developing an apparent polar wander path (APWP) for India in this poorly resolved period of Earth history.

2. Geological setting and previous work

The Archaean–early Proterozoic Bundelkhand craton (BC), commonly known as Bundelkhand Granite Massif (BGM) is a semicircular to triangular province that forms the northernmost part of the Indian peninsula (Fig. 2). It covers an area of ~29,000 km^2 and lies between latitudes 24°30′ and 26°00′N and longitudes 77°30′ E and 81°00′ E (Sharma, 1998). The BC is delimited to the west by the Great Boundary Fault, to the northeast by the Indo-Gangetic alluvial plains and to the south and southeast by the Narmada–Son lineament (Fig. 2). The southwestern margin is marked by relatively small outcrops of Deccan Basalt; additionally, Paleoproterozoic rocks of the Bijawar and Gwalior Groups are exposed in the SW and NE parts of the BC. The arcuate Vindhyan basin overlies the BC in the south and southeastern sections (Goodwin, 1991; Naqvi and Rogers, 1987; Pati et al., 2008; Meert et al., 2010). Sharma and Rahman (2000) divide the Bundelkhand craton into three lithotectonic units: (a) the ~3.5 Ga highly deformed granite-greenstone basement; (b) ~2.5 old multiphase granitoid plutons and associated quartz reefs; and (c) the mafic dykes and dyke swarms. The BGM represents a significant phase of felsic magmatism associated with a complex of pre-granite sedimentary rocks (Basu, 1986). The basement is represented by a highly deformed granite-greenstone terrane that consists of various enclaves of Archean gneisses, amphibolites, ultramafics, BIF's, tonalite–trondhjhemite-gneiss, marble, calc–silicate rocks, fuchsite quartzites and other metasediments (Roy et al., 1988; Basu, 1986; Sharma, 1998; Sinha Roy et al., 1998; Mondal and Zainuddin, 1996; Mondal et al., 2002). Three different phases of granitoid emplacement are identified in the BGM. In order of decreasing $^{207}Pb/^{206}Pb$ age, these granites include 2521 ± 7 Ma hornblende granite, 2515 ± 5 Ma biotite granite, and 2492 ± 10 leucogranites and constitute 80–90% of its exposed area (Gopalan et al., 1990; Wiedenbeck and Goswami, 1994; Wiedenbeck et al., 1996; Mondal et al., 1997, 1998, 2002; Malviya et al., 2004, 2006). Granitoid emplacement in the BC was followed by a number of minor intrusions including widespread pegmatitic veins, porphyry dykes and dyke swarms, and felsic units (rhyolites, dykes of rhyolitic breccias with angular enclaves of porphyries). Numerous quartz veins of varied size with mainly NNE–SSW and NE–SW trends are observed in parts of the BC representing episodic tectonically controlled hydrothermal activity (Pati et al., 1997, 2007).

The youngest phase of magmatism in the BGM is represented by mafic dykes and dyke swarms that traverse all the above lithologies. More than 700 mafic dykes are known to intrude the granitoid rocks of the BC (Pati et al., 2008). The majority of these dykes trend in a NW–SE direction, with subordinate ENE–WSW and NE–SW trending dykes including the ENE–WSW Great dyke of Mahoba (Basu, 1986; Mondal and Zainuddin, 1996; Mondal et al., 2002; Fig. 2). These mafic dykes are subalkaline to tholeiitic in composition and display continental affinity (Pati et al., 2008). The dykes are commonly exposed as a series of discontinuous and bouldery outcrops extending in length from few tens of meters to more than 17 km. The 'Great Dyke' of Mahoba has maximum strike length of ≥50 km (Figs. 2 and 3c and d). The dykes are generally non-foliated, relatively unaltered and exhibit sharp chilled contacts with the host granitoids (Fig. 3b). Basu (1986) distinguished at least three generations of dykes based on their cross-cutting relationships. The oldest, coarse grained NW–SE trending suite is cut by ENE–WSW and NE–SW trending medium-grained dykes that include small bodies and lenticles of an aphanitic dolerite. Numerous intermediate to felsic dykes are exposed in the west-central part of the massif between Jhansi and Jamalpur, including diorite porphyry, syenite porphyry and fine-grained syenite porphyry (Basu, 1986).

The ages for the Archaean rocks in the BGM are poorly constrained due to limited isotopic studies. The oldest rocks in the massif are associated with the TTG magmatism intruding the basement rocks and are assigned an age of 3503 ± 99 Ma (Rb–Sr isochron; Sarkar et al., 1996). Zircons from the basement gneiss yield an ion microprobe $^{207}Pb/^{206}Pb$ age of 3270 ± 3 Ma (Mondal et al., 2002). The Bastar, Dharwar and Aravalli cratons (Sarkar et al., 1993; Wiedenbeck et al., 1996) in peninsular India also contain coeval Archean basement rocks suggesting that these protocontinents played an important role in the earliest stages of nucleation of the Indian shield. The overall stabilization age for the massif has been interpreted to be ~2.5 Ga based on the $^{207}Pb/^{206}Pb$ ages of the granitoids (Meert et al., 2010; Crawford, 1975; Mondal et al., 1997, 1998, 2002; Roy and Kröner, 1996). The large scale granitic magmatism in the BC overlaps with similar events of granite magmatism and mineralization in adjacent Bastar (2490 ± 10 Ma; Stein et al., 2004) and Dharwar cratons (2510 Ma; Jayananda et al., 2000) indicating widespread granitic plutonism throughout much of the Indian shield at the Archean–Proterozoic boundary. Age control on the Bundelkhand mafic dykes is problematic and is loosely constrained to between ca. 2.1 and 1.5 Ga (Crawford, 1975; Crawford and Compston, 1970; Sarkar et al., 1997). More recent *in situ* $^{40}Ar/^{39}Ar$ laser ablation data yielded 2150 and 2000 Ma ages for mafic dykes (Rao, 2004; Rao et al., 2005) indicating two pulses of dyke emplacement, however, no details on the locations of the samples were provided in those publications. The majority of the laser spots for the *in situ* ^{40}Ar–^{39}Ar analysis were in the 2000 Ma range, suggesting that some of the older spot ages may suffer from excess argon within the samples.

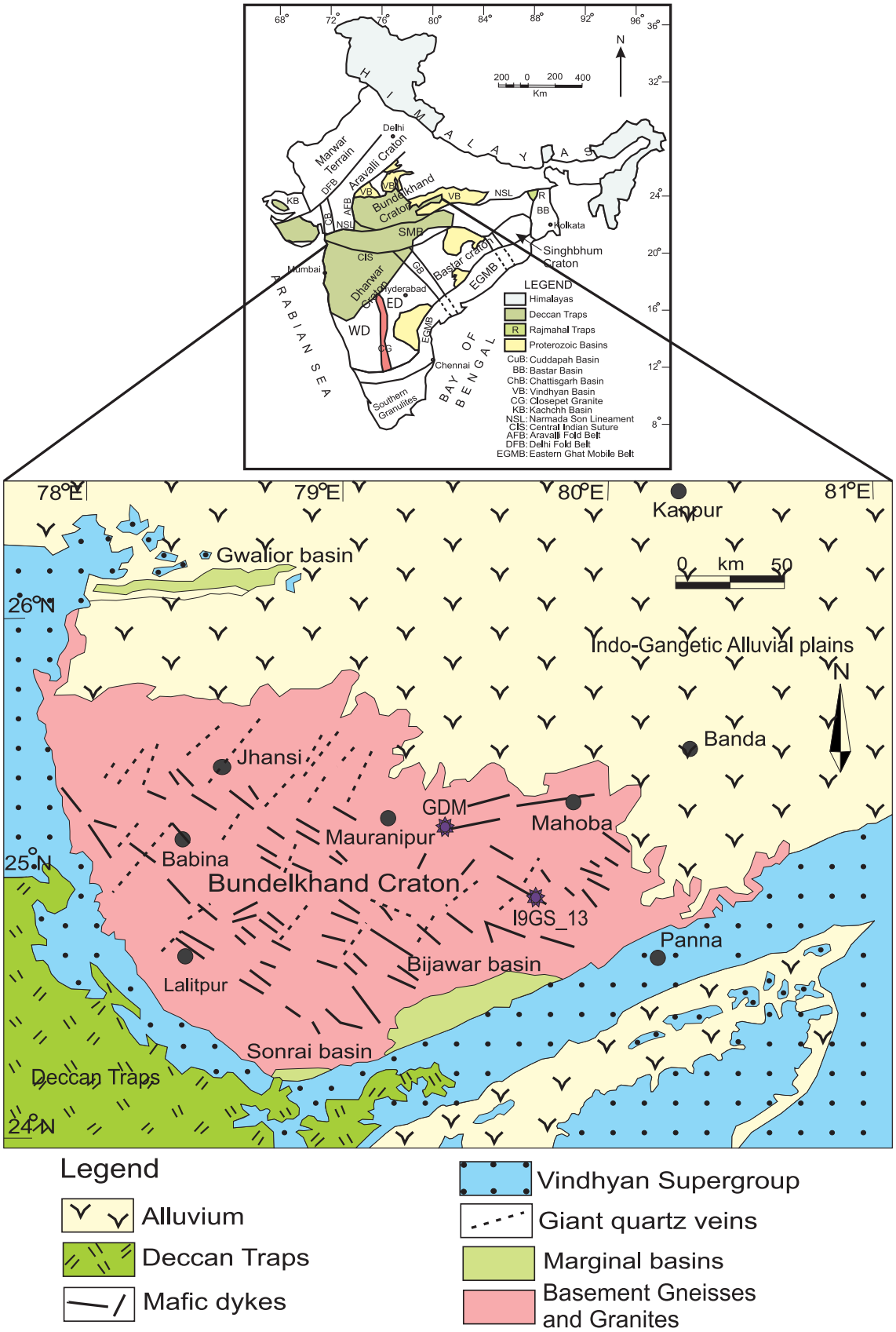

Fig. 2. Sketch map of the major units in the Bundelkhand craton, NW India (modified after Malviya et al., 2006). The asterisks on the map show the sites sampled for both paleomagnetic and geochronological analysis (NW–SE trending dyke I9GS_13 and ENE–WSW trending Great Dyke of Mahoba).

Fig. 3. (a) NW–SE trending dyke (I925) exposed in an outcrop ~50 km away from Mauranipur, M.P. (b) Granitic host rock at the same site I925 trellised by numerous mafic dykelets. (c and d) ENE–WSW trending dyke I923 exposed in a quarry in Mahoba district, Madhya Pradesh, Central India.

3. Sampling and methodology

3.1. Paleomagnetic methods

We sampled 27 sites (dykes) and collected a total of ~380 core samples from the mafic dykes intruding the Bundelkhand craton for paleomagnetic analysis (Fig. 2). Out of these, only 18 sites (dykes) yielded consistent results and are discussed in this paper (Table 1). All samples were drilled in the field using a water cooled portable drill. The samples were oriented using both sun and magnetic compass and readings were corrected for local magnetic declination and errors. Samples were returned to the University of Florida where they were cut into standard sized cylindrical specimens. These specimens were stepwise demagnetized by using both thermal and alternating field (AF) methods in order to identify the best treatment for isolating vector components within the samples. Alternating field demagnetization was conducted using a home-built AF demagnetizer and with fields up to 100 mT. Thermal demagnetization was conducted up to temperatures of 600 °C with an ASC-Scientific TD-48 thermal demagnetizer. Based upon the magnetic strength of the samples and instrument sensitivity the measurements were made on either a Molspin® spinner magnetometer or a 2G 77R Cryogenic magnetometer at the University of Florida. In samples that showed a very high initial NRM, samples were treated in liquid Nitrogen baths prior to thermal or AF treatment to remove any viscous multi-domain magnetism. Linear segments of the demagnetization trajectories were analyzed via principal component analysis using the IAPD software (Torsvik et al., 2000).

3.1.1. Rock magnetic tests

Curie temperature experiments were run on representative sample fragments from each site on a KLY-3S susceptibility Bridge with a CS-3 heating unit. Isothermal remanence acquisition (IRM) studies were performed on samples using an ASC-IM30 impulse magnetizer to further characterize the magnetic behavior.

3.2. Geochronological methods

Two samples from the NE–SW trending "Great Dyke of Mahoba" and five samples from the NW–SE trending older suite of mafic dykes from the Bundelkhand craton were processed for geochronology (Fig. 2). To ascertain the presence of uranium bearing phases, selected samples were thin sectioned and then imaged via scanning electron microscopy (SEM) for zircon/baddeleyite using the back scattered diffraction (BSD) method. Out of the dozen samples imaged, only two from the NE–SW trending younger suite (GDM and GDM-1) and four (including analyzed sample I9GS-13) from the NW–SE trending older suite displayed bright spots representative of zircon or baddeleyite, ranging in size between 2 and 100 μm (Fig. 4a and b). We pulverized sample I9GS_13 from the older suite and Mahoba dyke samples (GDM and GDM-1) for conventional methods of mineral extraction. Using standard gravity and magnetic separation techniques, the zircon grains were concentrated from pulverized samples at University of Florida. The samples were crushed, then disk milled and sieved to < 80-mesh grain size fraction. The fractions were then rinsed using Calgon (an anionic surfactant), followed by water table treatment with slow sample feed rates. This was followed by heavy liquid mineral separation with multiple agitation periods to reduce the number of entrapped grains in the lower density fraction. Finally, the samples were repeatedly passed through a Frantz Isodynamic magnetic separator up to a current of 1.0 Å (2–4° tilt). Approximately 15–20 clear, euhedral to nearly anhedral zircon grains and zircon fragments were handpicked from the two samples of the NE–SW trending younger Mahoba suite (GDM and GDM-1) and 25–35 subhedral to euhedral zircon grains from the NW–SE trending older suite (I9GS_13) under an optical microscope to ensure the selection of only the clearest grains and fragments of grains. Further handpicking of the grains reduced the number to only 7–8 good grains from the Mahoba dolerites and 10–15 grains from the I9GS-13 dyke sample. The grains were then mounted in resin and then polished to expose medial sections. Further sonication and cleaning of the plugs in 5% nitric acid (HNO_3) helped to remove any common-Pb surface contamination.

U/Pb isotopic analyses were conducted at the Department of Geological Sciences (University of Florida) on a Nu Plasma multi-collector plasma source mass spectrometer equipped with three ion counters and 12 Faraday detectors. The LA–ICPMC–MS is equipped with a specially designed collector block for simultaneous acquisition of ^{204}Pb (^{204}Hg), ^{206}Pb and ^{207}Pb signals on the ion-counting detectors and ^{235}Uand ^{238}U on the Faraday detectors (Mueller et al., 2008). Mounted zircon grains were laser ablated using a New-Wave 213 nm ultraviolet laser beam. During U/Pb analyses, the sample was decrepitated in a He stream and then mixed with Ar-gas for induction into the mass spectrometer. Background measurements were performed before each analysis for blank correction and contributions from ^{204}Hg. Each sample was ablated for ~30 s in an effort to minimize pit depth and fractionation. Data calibration and drift corrections were conducted using the FC-1 Duluth Gabbro zircon standard, long term reproducibility were 2% for ^{206}Pb/^{238}U (2σ) and 1% for ^{207}Pb/^{206}Pb (2σ) ages (Mueller et al., 2008). There was no significant ^{204}Pb detected in the samples and therefore, no common Pb correction was applied to the U–Pb data. Data reduction and correction were conducted using a combination of in-house software and Isoplot (Ludwig, 1999). Additional details can be found in Mueller et al. (2008).

4. Results

4.1. Geochronological results

The U/Pb ages from the zircon/zircon fragments were determined for the older NW–SE trending dyke sample I9GS_13 and the Great dyke of Mahoba samples GDM and GDM1. The dyke sample I9GS_13 yielded a number of well faceted zircons and zircon fragments suitable for U/Pb isotopic analysis. Eleven laser analyses on five different euhedral zircons yielded a concordia age of 1979 ± 8 Ma (2σ; MSWD (Conc. + Equival.) = 0.63; probability (Conc. + Equival.) = 0.90; Fig. 5a; Table 2a). This age is in rough agreement with reported *in situ* ^{40}Ar/^{39}Ar laser ablation data cited above (Rao, 2004; Rao et al., 2005). In addition, no crustal ages of 2.0 Ga are known from the Bundelkhand craton and no detrital component of this age has been identified in the adjacent Vindhyan and Marwar basins (Malone et al., 2008; Meert et al., 2010). Therefore, it is our interpretation that the 1978 Ma age reflects the crystallization age of the dyke. Ten analyses on four other fragmentary zircons from sample I9GS_13 yielded moderately discordant ^{207}Pb/^{206}Pb dates between 2777 and 2686 Ma (Fig. 5b; Table 2a). These results are broadly consistent with the ages of the basement rocks in the region (Mondal et al., 2002). Three analyses of a single zircon are slightly to moderately discordant, and the two least-discordant analyses agree to within uncertainty and yield a weighted mean ^{207}Pb/^{206}Pb date of 3254 ± 3 Ma (MSWD = 0.88) that is also a common age for basement rocks in the Bundelkhand craton (see Meert et al., 2010).

The two Mahoba dyke samples yielded only two well faceted grains and several fragments/tips of zircons (Fig. 4a). The regression derived from ^{207}Pb/^{206}Pb ratios from five laser analyses on three different zircon grains and zircon fragments/tips yielded a minimum concordant age of 1096 ± 19 Ma (2σ; MSWD = 0.3; Fig. 5c;

Table 1
Bundelkhand paleomagnetic results.

Site/study	Latitude/longitude	*N*/*n*	Dec	Inc	Kappa (κ)	α_{95}	VGP latitude	VGP longitude	dp/dm
Older Suite (NW–SE)									
Site I442	25.383°N, 78.536°E	5	141.0°	−0 9°	11.3	7.2°	47.2°N	325.7°E	3.7/7.3
Site I443[a]									
Dyke A	25.425°N, 78.672°E	2	139.0°	−12.6°	70.0	11.1°	46.5°N	329.8°E	5.8/11.3
Dyke B	25.425°N, 78.672°E	4	141.4°	5.8°	70.0	11.1°	43.2°S	137.1°E	5.6/11.1
Dyke C[b]	25.425°N, 78.672°E	2	339.0°	−21°	70.0	11.1°	48.5°S	110.5°E	6.1/11.7
Site I444	25.408°N, 78.669°E	7	174.0°	−14.8°	16.0	15.5°	71.4°N	277.3°E	8.1/15.9
Site I454	25.147°N, 80.050°E	7	156.5°	−17.3°	50.0	8.6°	62.4°N	318.2°E	4.6/8.9
Site I455	24.935°N, 79.902°E	18	149.0°	−21°	47.3	5.1°	57.6°N	330.6°E	2.8/5.5
Site I925	24.946°N, 79.911°E	34	151.3°	−19.5°	34.0	4.3°	59.1°N	326.5°E	2.3/4.5
Site I927	25.017°N, 80.475°E	27	167.5°	−15.9°	42.0	4.3°	69.3°N	297.6°E	2.3/4.4
Site I929	25.192°N, 80.464°E	9	168.2°	−10.3°	107	5.0°	67.1°N	291.8°E	2.6/5.1
Site I930	25.189°N, 80.469°E	16	164.0°	−13.2°	71.3	4.4°	66.1°N	302.7°E	2.3/4.5
Site I931	25.286°N, 79.919°E	10	152.9°	−8.8°	46.2	7.2°	56.8°N	315.3°E	3.7/7.3
Mahoba dykes (ENE–WSW)									
Site I451	25.284°N, 79.851°E	23	14.6°	−31.7°	25.0	6.1°	45.3°S	59.5°E	3.8/6.9
Site I452	25.284°N, 79.851°E	13	27.6°	−48.7°	232.0	2.7°	29.1°S	52.1°E	2.3/3.6
Site I923	25.184°N, 79.401°E	20	14.2°	−37.0°	125.0	3.3°	42.2°S	61.2°E	2.3/3.9
Site I924 (great circles)	25.301°N, 79.934°E	10	40.7°	−29.2°	–	2.8°	33.1°S	31.0°E	1.7/3.1
NE–SW (third dyke suite)									
Site I448	25.134°N, 79.750°E	20	200.0°	60.0°	42.4	14.3°	21.5°S	63.3°E	16.3/21.6
Site I928	25.052°N, 80.486°E	20	175.0°	68.0°	48.6	4.7°	13.8°S	83.5°E	6.6/7.9
Overall mean–older (NW–SE)	25.00°N,80°E	141/12	155.3°	−7.8°	21.4	9.6°	58.5°N	312.5°E	4.9/9.7
Overall mean–Mahoba (ENE–WSW)	25.17°N,79.5°E	76/4	24.7°	−37.9°	35.9	15.5°	38.7°S	49.5°E	9.5/16.3

N: number of samples used; *n*: number of dykes/sites; Dec: declination; Inc: inclination; κ: kappa precision parameter; α_{95}: cone of 95% confidence about the mean direction; VGP: virtual geomagnetic pole.

[a] Dyke A, B and C are 3 small dykes from Site I443 with Dyke C.

[b] Showing reverse polarity.

Table 2a
Geochronological Results from the Bundelkhand older suite of dykes (I9GS_13).

Ratios							Ages							
Grain	$^{207}Pb/^{206}Pb$	±2σ	$^{206}Pb/^{238}U$	±2σ	$^{207}Pb/^{235}U$	±2σ	$^{206}Pb/^{238}U$ (Ma)	±2σ	$^{207}Pb/^{235}U$ (Ma)	±2σ	$^{207}Pb/^{206}Pb$ (Ma)	±2σ	% Disc	RHO
I9GS_13_2	0.1222	0.0012	0.34907	0.0179	5.88	0.30	1930	43	1959	22	1989	8	3	0.98
I9GS_13_6	0.1230	0.0016	0.35774	0.0239	6.07	0.42	1971	57	1985	30	2000	12	1	0.98
I9GS_13_7	0.1218	0.0026	0.36297	0.0223	6.10	0.40	1996	53	1990	28	1983	19	−1	0.95
I9GS_13_8	0.1210	0.0014	0.36787	0.0208	6.14	0.36	2019	49	1995	25	1970	10	−3	0.98
I9GS_13_9	0.1212	0.0012	0.37220	0.0221	6.22	0.38	2040	52	2007	26	1975	9	−3	0.98
I9GS_13_10	0.1220	0.0016	0.36876	0.0188	6.20	0.32	2023	44	2004	23	1985	11	−2	0.97
I9GS_13_11	0.1215	0.0012	0.35601	0.0164	5.96	0.28	1963	39	1970	20	1978	9	1	0.98
I9GS_13_14	0.1218	0.0012	0.35741	0.0198	6.00	0.34	1970	47	1976	24	1983	9	1	0.98
I9GS_13_15	0.1214	0.0012	0.35357	0.0157	5.92	0.26	1952	37	1964	20	1977	9	1	0.98
I9GS_13_16	0.1211	0.0014	0.35077	0.0178	5.86	0.28	1938	39	1955	21	1972	10	2	0.97
I9GS_13_17	0.1213	0.0012	0.35355	0.0163	5.91	0.30	1951	42	1963	22	1975	9	1	0.98
I9GS_13_21	0.1883	0.0008	0.45398	0.0221	11.79	0.58	2413	98	2588	45	2728	7	12	0.99
I9GS_13_23	0.1928	0.0007	0.47373	0.0190	12.59	0.51	2500	83	2649	38	2766	6	10	0.99
I9GS_13_24	0.1939	0.0008	0.46927	0.0187	12.55	0.50	2480	82	2646	37	2776	6	11	0.99
I9GS_13_26	0.2572	0.0020	0.47423	0.0696	16.82	2.47	2502	301	2924	136	3230	12	23	1.00
I9GS_13_27	0.2611	0.0007	0.63422	0.0162	22.83	0.59	3166	64	3220	25	3253	4	3	0.99
I9GS_13_28	0.2615	0.0008	0.56674	0.0566	20.44	2.04	2894	231	3112	95	3256	5	11	1.00
I9GS_13_30	0.1941	0.0007	0.50044	0.0099	13.39	0.27	2616	43	2708	19	2777	6	6	0.98
I9GS_13_31	0.1900	0.0007	0.48971	0.0130	12.83	0.34	2569	56	2667	25	2743	6	6	0.99
I9GS_13_33	0.1864	0.0008	0.48857	0.0105	12.56	0.28	2564	45	2647	21	2711	7	5	0.98
I9GS_13_34	0.1896	0.0012	0.45310	0.0204	11.85	0.54	2409	90	2592	42	2739	10	12	0.99
I9GS_13_35	0.1837	0.0006	0.46585	0.0121	11.80	0.31	2465	53	2588	24	2686	6	8	0.99
I9GS_13_37	0.1852	0.0009	0.47595	0.0122	12.16	0.32	2510	53	2616	24	2700	8	7	0.98
I9GS_13_38	0.1888	0.0016	0.49585	0.0112	12.91	0.31	2596	48	2673	23	2732	14	5	0.98

Table 2b
Geochronological results from the Mahoba dykes (GDM and GDM1).

Ratios							Ages							
Grain	$^{207}Pb/^{206}Pb$	±2σ	$^{206}Pb/^{238}U$	±2σ	$^{207}Pb/^{235}U$	±2σ	$^{206}Pb/^{238}U$ (Ma)	±2σ	$^{207}Pb/^{235}U$ (Ma)	±2σ	$^{207}Pb/^{206}Pb$ (Ma)	±2σ	% Disc	RHO
GDM_5a	0.07697	0.0006	0.17605	0.0051	1.868	0.06	1046	28	1070	20	1120	17	7	0.96
GDM_6a	0.07697	0.0007	0.17509	0.0040	1.858	0.05	1041	22	1066	16	1120	18	7	0.93
GDM_7a	0.07671	0.0006	0.17551	0.0041	1.856	0.05	1043	23	1066	16	1114	16	6	0.95
GDM_8a	0.07654	0.0006	0.17623	0.0041	1.860	0.05	1047	23	1067	16	1109	17	6	0.94
GDM_18a	0.07631	0.0006	0.18242	0.0041	1.919	0.05	1081	22	1088	16	1103	16	2	0.94

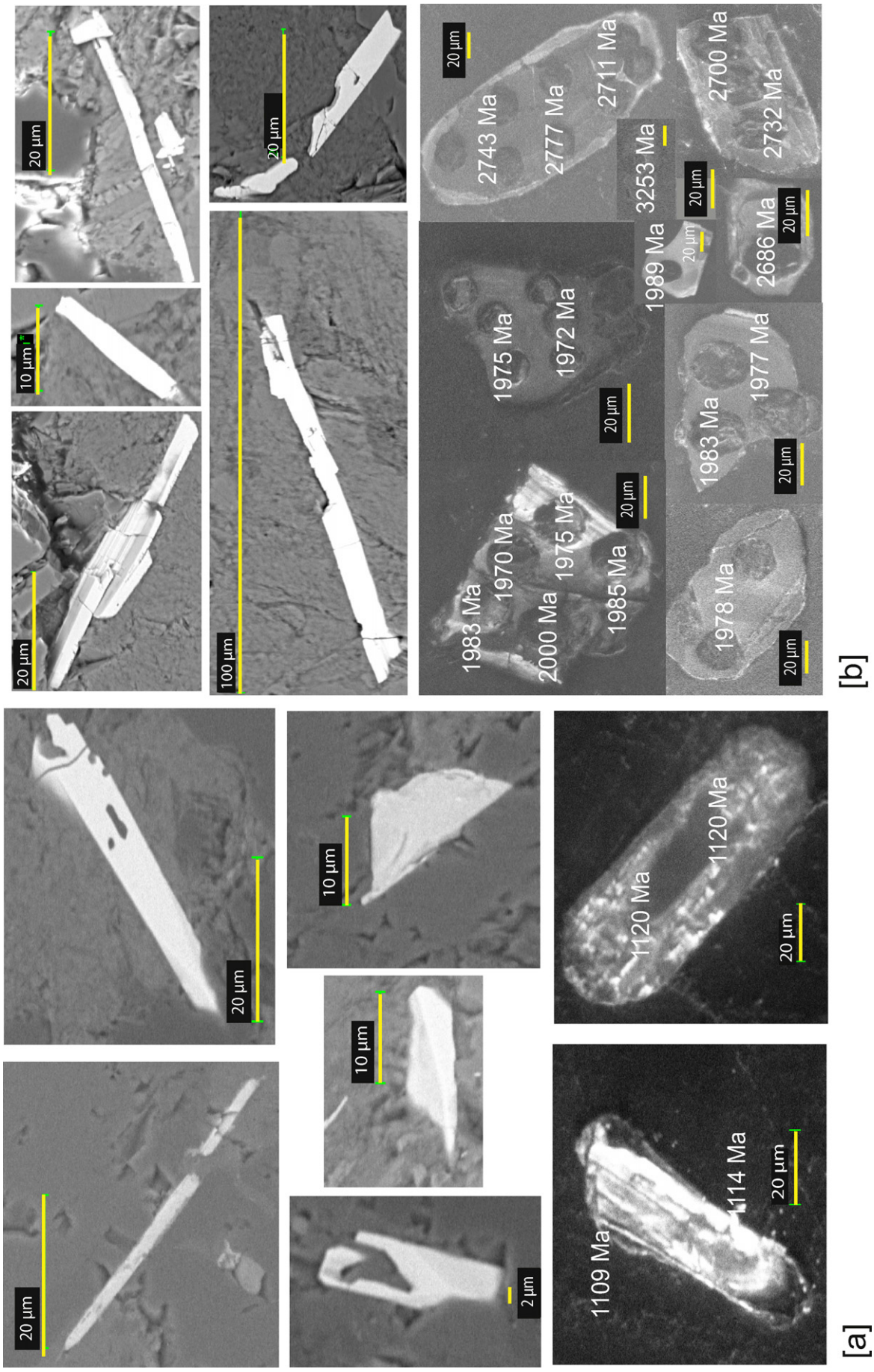
20 µm
10 µm
100 µm
2 µm
1109 Ma
1114 Ma
1120 Ma
1120 Ma
1983 Ma
1970 Ma
2000 Ma
1975 Ma
1985 Ma
1975 Ma
1972 Ma
1978 Ma
1983 Ma
1977 Ma
1989 Ma
3253 Ma
2686 Ma
2743 Ma
2777 Ma
2711 Ma
2732 Ma
2700 Ma
[a]
[b]

Table 2b). The weighted mean $^{207}Pb^*/^{206}Pb^*$ age for these five analysis yielded an age of 1113 ± 7 (2σ; MSWD = 0.75; probability of fit = 0.56; Fig. 5d; Table 2b).

4.2. Paleomagnetic results

The paleomagnetic directions/statistics for the individual NW–SE, ENE–WSW and NE–SW trending Bundelkhand mafic dykes are listed in Table 1. Three distinct paleomagnetic directions were recorded for the doleritic dykes suggesting three episodes of dyke emplacement within the BC varying in space and time. A stable uni-vectorial demagnetization trend was observed for a majority of these samples during thermal/AF treatments. The samples show discrete unblocking temperatures between 550 and 570 °C. The 'B' samples treated with AF demagnetization show gradual decrease in their magnetic intensity and behave consistently over a wide range of coercivity spectrum (Fig. 6b and d).

The NRM intensities for the ENE–WSW trending Mahoba dyke samples range between 0.4 and 0.1 A/m (Fig. 6a and b). The intensity plots yielded unblocking temperatures between 550 and 560 °C during thermal demagnetization while AF demagnetization yielded wide coercivity spectrum, consistent with low-Ti magnetite as the main carrier of magnetization (Fig. 6a and b). The overall mean direction calculated from four ENE–WSW Mahoba dykes has a declination = 24.7° and inclination = −37.9° (κ = 36; α_{95} = 15.5°) and a resultant virtual geomagnetic pole (VGP) at 38.7°S and 49.5°E (dp/dm = 9.5°/16.3°; (Fig. 9a).

Fifteen dykes were sampled from the older NW–SE trending suite and twelve yielded consistent stable paleomagnetic directions (Table 1). The NRM intensities for these samples vary from 0.44 to 0.11 A/m. Fig. 6c and d shows the demagnetization behavior of two pilot dyke specimens to the thermal and AF treatments. The mean paleomagnetic direction obtained from these 12 dykes has a declination = 155.3° and inclination = −7.8° (κ = 21; α_{95} = 9.6) after inverting one reverse polarity dyke I443 C (Fig. 9b; Table 1). The overall paleomagnetic pole calculated from these twelve dykes falls at 58.5°N and 312.5°E (dp/dm = 6.6°/7.9°).

In addition to these two directions from the NW–SE and ESE–WNW dykes, a third distinct steep paleomagnetic direction was obtained from two of the NE–SW trending dykes. The overall mean direction calculated for these two dykes has a declination = 189.3° and inclination = +64.5° (Fig. 9c). This is suggestive, though not conclusive, evidence for a third episode of dyke emplacement within the BC.

The Bundelkhand granitic host rock samples were also collected at sites I925 and I927 with the intent to perform a baked contact test. Unfortunately, the vast majority of the granites were dominated by multi-domain magnetite and no consistent directions were obtained with one exception. At site I925 numerous mafic dykelets were observed trellising the granitic host rock (Fig. 3b). These granitic samples in contact with the mafic dykelets were taken about 1.5″ away from the main dyke (Fig. 3a) and stable paleomagnetic directions were obtained for the host granites that were similar to the main dyke I925 (Fig. 7a and b). In addition, one of the dykes (site I443C) is of opposite polarity to the characteristic magnetization observed in the majority of dykes (declination = 339° and inclination = −21°; κ = 70; α_{95} = 11.1). While not conclusive, the partial baked contact test, the dual polarity signal and the fact that the three suites of dykes (NE–SW, ENE–WSW and NW–SE) yield distinct paleomagnetic directions support a primary magnetization in the NW–SE trending older suite of dykes and negates arguments for a younger remagnetization in the region.

4.2.1. Rock magnetic results

Representative results of thermomagnetic analysis (susceptibility vs. temperature) of ENE–WSW and NW–SE trending dyke samples are shown in Fig. 8(a–d). The heating and cooling curves of magnetic susceptibility for the ENE–WSW trending Mahoba dykes as shown in Fig. 8a and c display two magnetic phases. The heating curves show a prominent peak centered close to 250–300 °C and susceptibility drop above 300° C, indicating the likely existence of pyrrhotite. A rapid decrease in the magnetic susceptibility around 550–575 °C indicates the existence of magnetite (Fig. 8a and c). The cooling curve shows higher susceptibility which is probably caused by the ex-solution and conversion of Ti-magnetite to pure magnetite (Fig. 8a and c).

The rock magnetic studies on the dominantly occurring NW–SE trending older suite of dykes show nearly reversible Curie temperature runs characteristic of magnetite (Fig. 8b and d). The heating Curie temperature T_cH of dyke sample I927-12 is 572.8 °C, and the cooling Curie temperature T_cC is 567.5 °C (Fig. 8d). IRM curves along with back field coercivity of remanence from both these ENE–WSW and NW–SE trending mafic dykes also indicate magnetite as the principal magnetic carrier in the samples. A rapid rise in intensity near saturation at ~0.25 to 0.3 T was observed for majority of the dyke samples and their magnetization remains constant at higher fields, up to the highest applied field of 1.2 T. The values for the back field coercivity of remanence ranges between 0.07 and 0.1 mT (Fig. 8e and f).

5. Discussion

5.1. 1.1 Ga paleomagnetism

The VGP calculated for the ENE–WSW trending Mahoba dykes of the Bundelkhand craton is significant in terms of its age and the direction. The U–Pb zircon age of 1113 ± 7 Ma for Mahoba dykes falls in the same time bracket as the Majhgawan kimberlite that intrudes both the Lower Vindhyan sequence (~1.6 Ga) and the Baghain sandstone of the Kaimur Group (Upper Vindhyan). Gregory et al. (2006) dated Majhgawan kimberlite at 1073 ± 13.7 Ma via ^{40}Ar–^{39}Ar analysis of phlogopite phenocrysts and obtained a virtual geomagnetic pole at 36.8°S, 32.5°E (dp = 9°; dm = 16.6°; also see Miller and Hargraves, 1994) that is statistically indistinguishable from the virtual geomagnetic pole calculated for the Mahoba dyke swarm in this study (Fig. 10). Malone et al. (2008) conducted a paleomagnetic study on the Bhander–Rewa Groups (Upper Vindhyan) and obtained a mean paleomagnetic pole at 44°S, 34.0°E (A95 = 4.3). We note that the VGP's of the Mahoba dykes generated in this study and the penecontemporaneous Majhgawan kimberlite are nearly identical to the paleomagnetic poles obtained from the Bhander–Rewa Groups in the Upper Vindhyan sequence (Fig. 10).

Azmi et al. (2008) argue that the paleomagnetic data from the Majhgawan kimberlite and the Bhander–Rewa sequence are indeed age-equivalent and late Neoproterozoic in age, but that the Majhgawan phlogopites crystallized at depth some 400 million years earlier. We acknowledge that the presence of similar magnetizations in three different units in close proximity may also raise concern about the possibility of remagnetization. However, we note that there is no reported ~1.1 Ga remagnetization event within or in the vicinity of the Bundelkhand craton.

Fig. 4. (a) Backscattered electron (BSE) and cathodoluminescence (CL) images of selected zircons/uranium bearing minerals from ENE–WSW trending Mahoba dykes. Scale bars in μm. (b) Backscattered electron (BSE) and cathodoluminescence (CL) images of selected zircons/uranium bearing minerals from NW–SE trending dykes. Bar length corresponds to 10–100 μm.

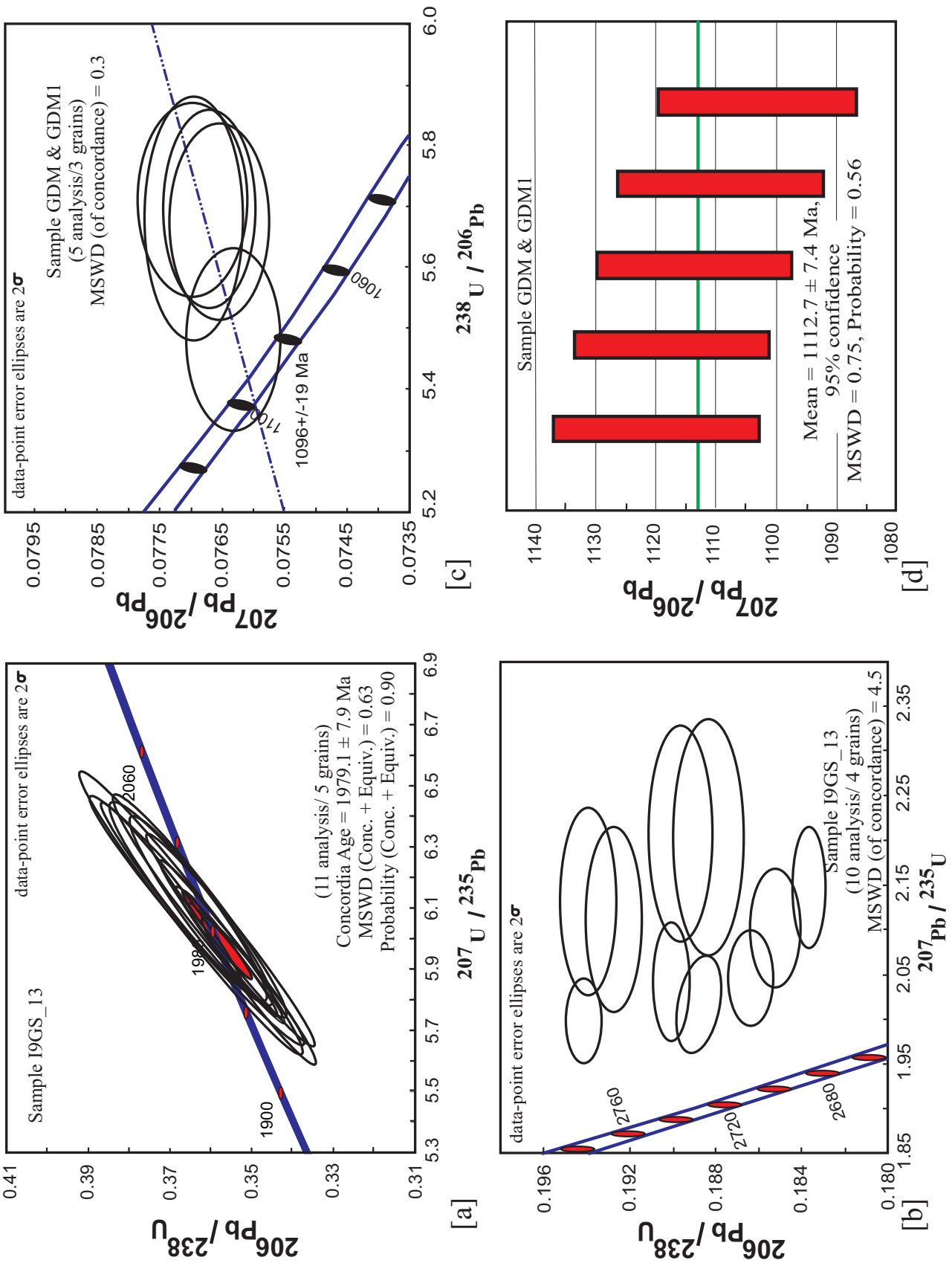

Fig. 5. (a) Concordia diagram for the 11 spots from five concordant zircon/baddeleyite grains and tips from sample I9GS_13 yielding an age of 1979.1 ± 7.9 Ma (2σ; MSWD = 0.63; probability = 0.90). (b) Tera–Wasserburg plot obtained from 10 analyses on a population of four fragmentary zircons/baddeleyites from NW–SE trending dyke sample I9GS_13 yielding moderately discordant $^{207}Pb/^{206}Pb$ dates between 2777 and 2686 Ma (2σ; MSWD = 4.5) (c) Tera–Wasserburg concordia intercept age of 1096 ± 19 Ma (2σ; MSWD = 0.3) derived from the regression through the uncorrected data from the $^{207}Pb/^{206}Pb$ for the five analysis on three zircon grains and tips from sample GDM and GDM1 (d) The weighted mean $^{207}Pb^*/^{206}Pb^*$ age for the five analysis from sample GDM and GDM1 yielded an age of 1113 ± 7 (2σ; MSWD = 0.75; probability of concordance = 0.56).

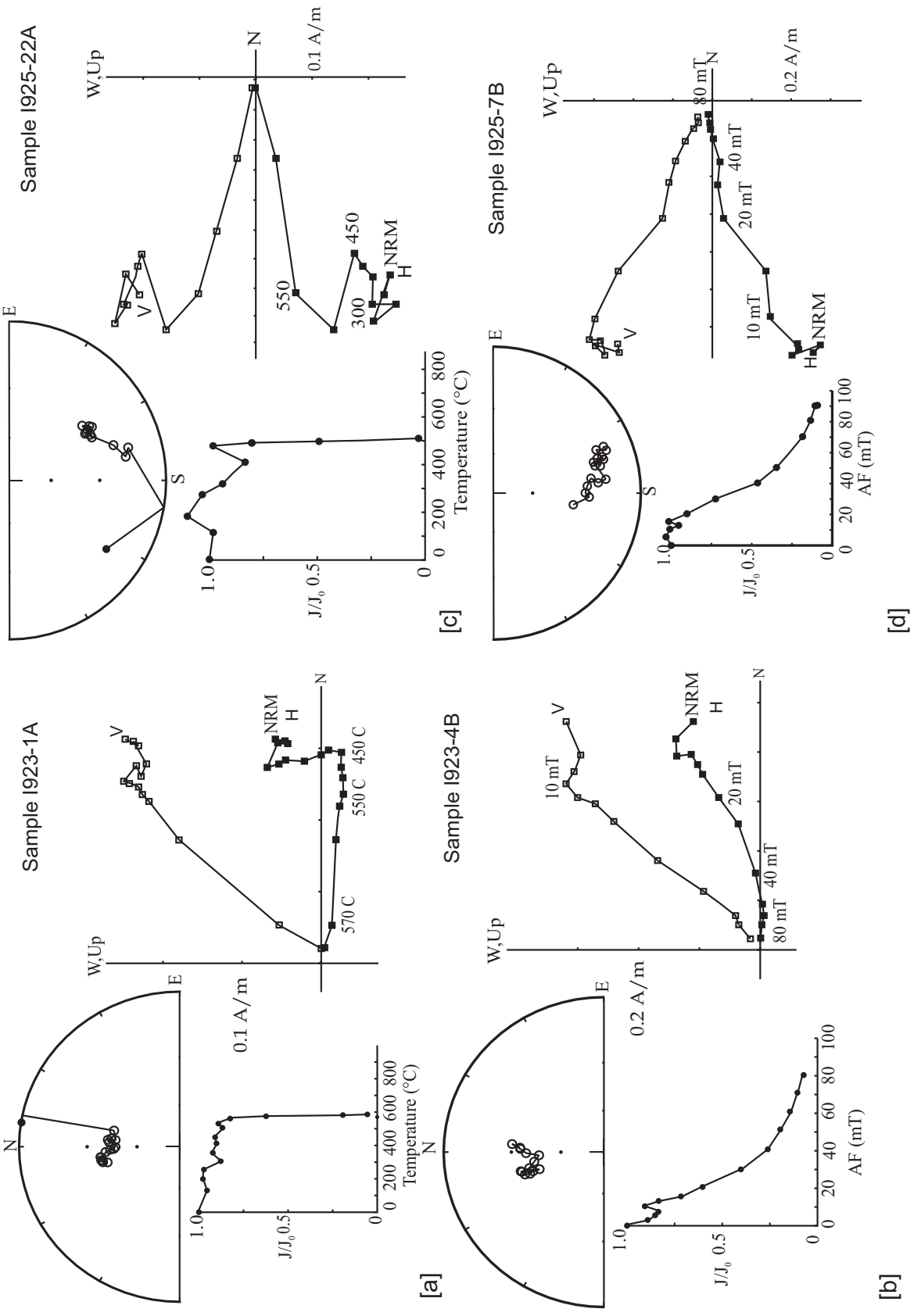

Fig. 6. Orthogonal vector plots from the NW–SE and ENE–WSW trending dykes of the Bundelkhand craton showing typical characteristic remanent magnetization directions. (a) Thermal demagnetization behavior of ENE–WSW trending dyke sample I923-1A. (b) Alternating field demagnetization behavior of ENE–WSW trending dyke specimen I923-4B. (c) Thermal demagnetization behavior of NW–SE trending dyke sample I925-22A. (d) Alternating field demagnetization behavior of NW–SE trending dyke sample I925-7B. Solid squares represent projections on the horizontal plane indicated by 'H'; open squares represent projection onto a vertical plane indicated by 'V'.

Additional support for the primary nature of magnetization is found in both Upper Vindhyan sequence and the NW–SE trending older suite of Bundelkhand dykes. Upper Vindhyan sedimentary units show at least eleven geomagnetic reversals supporting a primary magnetization in these rocks. Similarly, the presence of partial baked contact test yielded by the granitic host rock samples traversed by the mafic dykelets at site I925 (Fig. 7e and f) and the dual polarity magnetization shown by one of the dykes (site I443C) support a primary magnetization in the NW–SE trending older suite of Bundelkhand dykes.

5.1.1. Age implications for the Bhander–Rewa sequence of the Upper Vindhyan

The age of deposition in Vindhyan basin located to the south of the Bundelkhand Craton (Fig. 1) in the northern Indian peninsular shield, has been debated for over 100 years (Oldham, 1893; Auden, 1933; Crawford and Compston, 1970; Venkatachala et al., 1996; Malone et al., 2008; Azmi et al., 2008). The onset of sedimentation in the lower Vindhyan Supergroup is generally well constrained at around 1.6–1.8 Ga by radiometric data (Rasmussen et al., 2002a,b; Ray et al., 2002, 2003 Sarangi et al., 2004; Kumar, 2001); however the age of the Upper Vindhyan is still enigmatic and highly contentious due to lack of targets suitable for geochronology, controversial fossil finds and poorly constrained global stable isotopic correlations (Vinogradov et al., 1964; Crawford and Compston, 1970; Paul et al., 1975; Srivastava and Rajagopalan, 1988; Chakrabarti, 1990; Smith, 1992; Kumar and Srivastava, 1997; Kumar et al., 2002; De, 2003, 2006; Ray et al., 2002, 2003; Rai et al., 1997; Gregory et al., 2006; Malone et al., 2008; Azmi et al., 2008).

The Upper Vindhyan sedimentary rocks were typically correlated with the Marwar Supergroup (Rajasthan); sequences in the Salt Range of Pakistan and with the Krol–Tal Group of the Lesser Himalayas (McElhinny et al., 1978; Klootwijk et al., 1986; Mazumdar and Banerjee, 2001). These correlations, however, are based on somewhat similar lithologies and the proximity of the undeformed Marwar and Upper Vindhyan strata.

The lithologic comparisons between these units are rather problematic. For example, the evaporite deposits are prevalent within the Marwar and Salt Ranges, but absent in the Upper Vindhyan sequence. Malone et al. (2008) examined detrital zircon suites from both the Upper Vindhyan sedimentary rocks in Rajasthan and the nearby Marwar Supergroup. The $^{207}Pb/^{206}Pb$ age distribution observed in the detrital zircon analysis of the Upper Bhander sandstone yielded several noteworthy peaks between 1850 and 1050 Ma (Malone et al., 2008). In contrast, detrital zircons analyzed from the Sonia and Girbarkhar sandstone of the Marwar Supergroup yielded age peaks in the 840–920 Ma range, a component completely absent in the Upper Bhander sandstone of the Vindhyan Supergroup. Hence, the results from the detrital zircon geochronology suggest that previous correlations between the two depositional sequences are incorrect. Malone et al. (2008) hypothesized that the closure age of the Upper Vindhyan sedimentation was no younger than 1.0 Ga based on their paleomagnetic study on the Bhander–Rewa Groups of the Upper Vindhyan and the detrital zircon work on Bhander–Rewa units and the Marwar Supergroup. Additional support for a Late Mesoproterozoic closure age came from a paleomagnetic/geochronological study of the Majhgawan kimberlite (Gregory et al., 2006).

The paleomagnetic and geochronological data from the Mahoba dykes generated in this study is germane to the discussion of the sedimentation ages in the Upper Vindhyan basin. The VGP obtained for the ~1113 Ma Mahoba dykes (37.8°S, 49.5°E) is nearly identical to the mean paleomagnetic pole from the Bhander–Rewa Groups and the Majhgawan kimberlite (Fig. 10; see discussion above). Our interpretation of the Mahoba paleomagnetic and geochronological results therefore lends additional support to the proposal of Malone et al. (2008) and Gregory et al. (2006) that the closure of sedimentation in the Upper Vindhyan sequence is older than ~1.0 Ga.

5.1.2. India in Rodinia supercontinent at 1100 Ma

The Late Mesoproterozoic (ca. 1100 Ma) has been postulated as the time interval for the formation of the supercontinent Rodinia (McMenamin and McMenamin, 1990; Dalziel, 1991; Moores, 1991; Hoffman, 1991). The existence of Rodinia is supported by the presence of a number of 1300–900 Ma old orogenic/mobile belts (Dewey and Burke, 1973) and associated geologic links between the various cratonic nuclei (Young, 1995; Dalziel, 1997; Rainbird et al., 1998; Karlstrom et al., 1999; Sears and Price, 2000; Dalziel et al., 2000). However, the geometry/paleogeography and duration of the Rodinia supercontinent remains extremely fluid and controversial due to a paucity of well dated, high quality paleomagnetic poles from various continental blocks forming the supercontinent (Weil et al., 1998; Meert and Powell, 2001; Meert, 2001; Meert and Torsvik, 2003; Li et al., 2008).

One of the outcomes of this study is our ability to constrain the paleoposition of Indian sub-continent in Rodinia configuration at ~1.1 Ga. The recent paleomagnetic and geochronological studies from the Majhgawan kimberlite (Gregory et al., 2006) and Bhander–Rewa Groups of Upper Vindhyan (Malone et al., 2008) provided high quality poles to constrain the paleogeographic position of India at 1.1 Ga.

There are a number of paleomagnetic poles available from other elements of the Rodinia supercontinent that are more or less coeval with those from India. Considering the East Gondwana elements, the key pole for this interval in Australia is the ~1070 Ma doleritic rocks of Bangemall sills (Wingate et al., 2002). The Bangemall pole achieves a score of $Q = 7$ in the reliability scheme of Van der Voo (1990).

The paleogeographic position for Laurentia is based on the combined mean paleomagnetic data from the Portage Lake volcanics and Keweenawan dykes (Pesonen et al., 2003; Swanson-Hysell et al., 2009). Based on the extensive field and laboratory tests these poles are inferred to be primary and have precise zircon/baddeleyite U–Pb dates of 1095 Ma (Portage Lake Volcanics) and ~1109 Ma (Keweenawan volcanics), respectively (Halls and Pesonen, 1982; Davis and Sutcliffe, 1985; Goodge et al., 2008). More recently, Swanson-Hysell et al. (2009) provided high resolution paleomagnetic data from a series of well-dated basalt flows at Mamainse Point, Ontario, in the Keweenawan Rift and suggested that the previously documented reversal asymmetry for these volcanic rocks is an artefact of the fast motion of the Laurentian plate towards the equator at this interval (also see Meert, 2009). The combined mean of the Portage Lake volcanics and the Keweenawan dolerites pole places Laurentia at intermediate paleolatitudes in our ~1.1 Ga reconstruction.

There are two paleomagnetic poles available from the Baltica between ~1100 and 1123 Ma. Most of the Rodinia reconstructions at ~1100 Ma utilize the paleomagnetic data from the Bamble intrusions in southern Norway to constrain the position of Baltica (Brown and McEnroe, 2004; Stearn and Piper, 1984). A Sm/Nd metamorphic age of 1095 Ma has been reported for the Bamble intrusive rocks intruding the high grade granulite facies. Recently, Salminen et al. (2009) reported a virtual geomagnetic pole for the Baltica from their paleomagnetic and rock magnetic studies on the well dated 1122 ± 7 Ma (U–Pb age; Lauerma, 1995) Salla diabase dykes in northeastern Finland. The palaeolatitudinal position of Baltica constrained by the Bamble intrusive poles and the Salla dykes VGP indicate a latitudinal difference of almost 90°. This would require an unusually rapid southward drift of the Baltica plate for the short time interval of ~28 Ma. However, the Salla diabase dyke pole is highly tentative and requires additional verification due

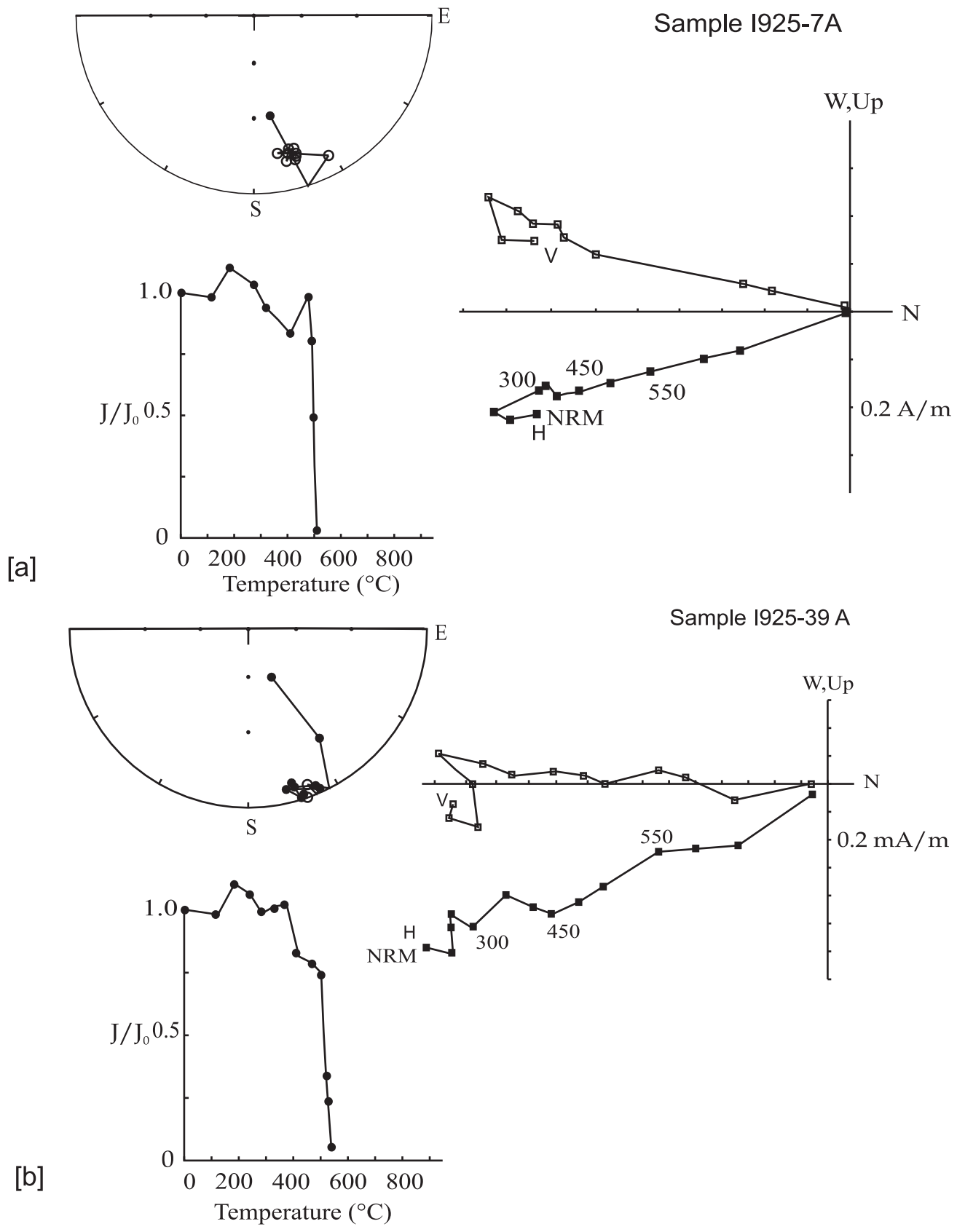

Fig. 7. Baked contact test on NW–SE trending dyke I925. (a) Thermal demagnetization behavior of the dyke specimen I925-7A. (b) Thermal demagnetization behavior of the granitic host rock specimen I925-39A about 1.5 m away from the main dyke showing similar directions as the main dyke.

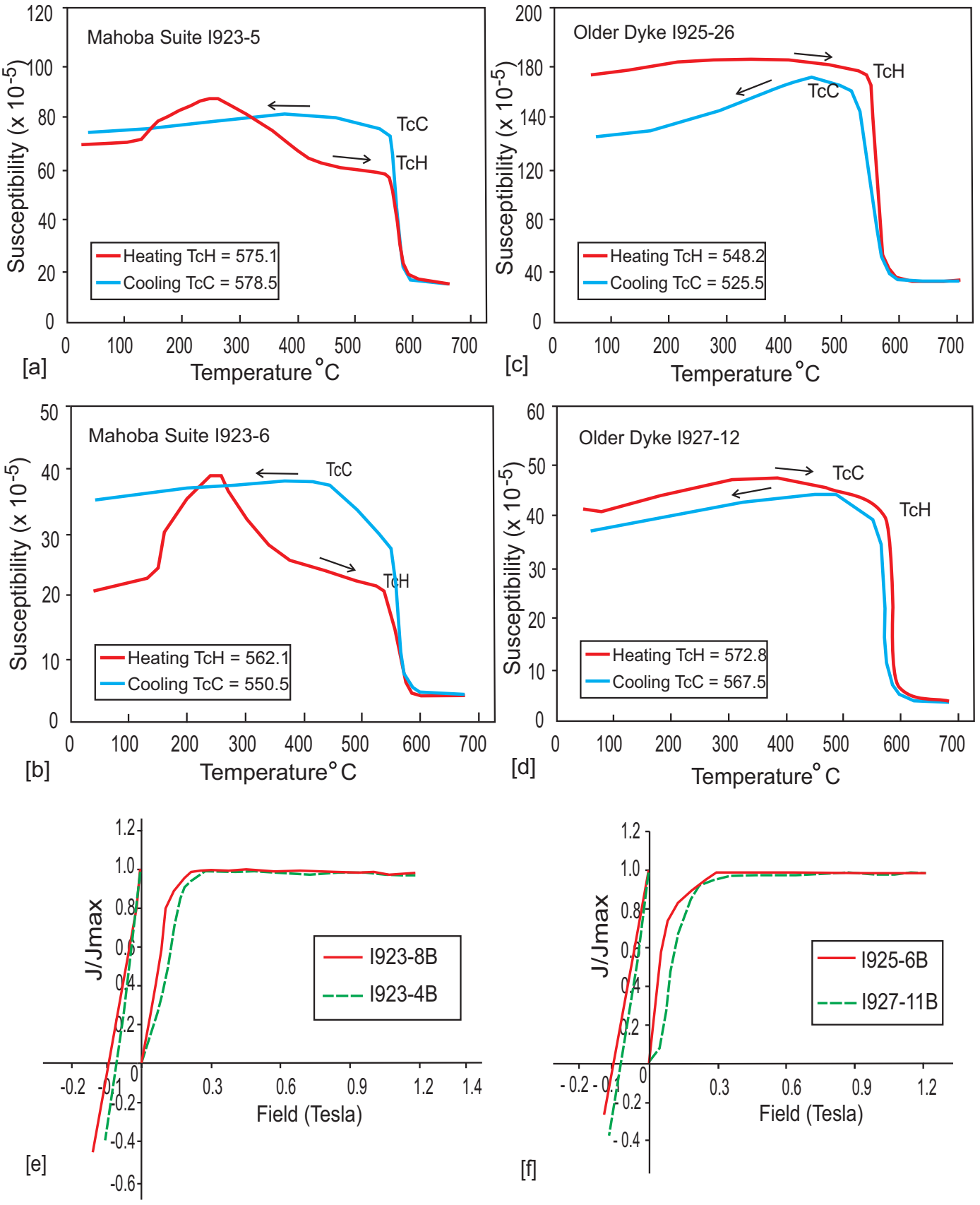

Fig. 8. (a and b) Curie temperature runs for ENE–WSW trending dyke samples I923-5 and 6. Sample I923-5a shows Heating curie temperature (T_cH) of 575.1 °C and Cooling curie temperature (T_cC) of 578.5 °C and I923-6 shows T_cH = 562.1 °C and T_cC = 550.5 °C. (c and d) Curie temperature runs for the NW–SE trending older dyke suite samples I925-26 (T_cH = 548.2 °C and T_cC = 525.5 °C) and I927-12 (T_cH = 572.8 °C and T_cC = 567.5 °C). (e) Isothermal remanence magnetization (IRM) acquisition and back field demagnetization behavior of the two ENE–WSW dyke specimens I923-4B and (B). (f) IRM acquisition and back field demagnetization behavior of two NW–SE dyke samples I925-6B and 11B. All samples saturate at about 0.25–0.3 T. Coercivity of remanence values ranged from 0.07 to 0.1 T.

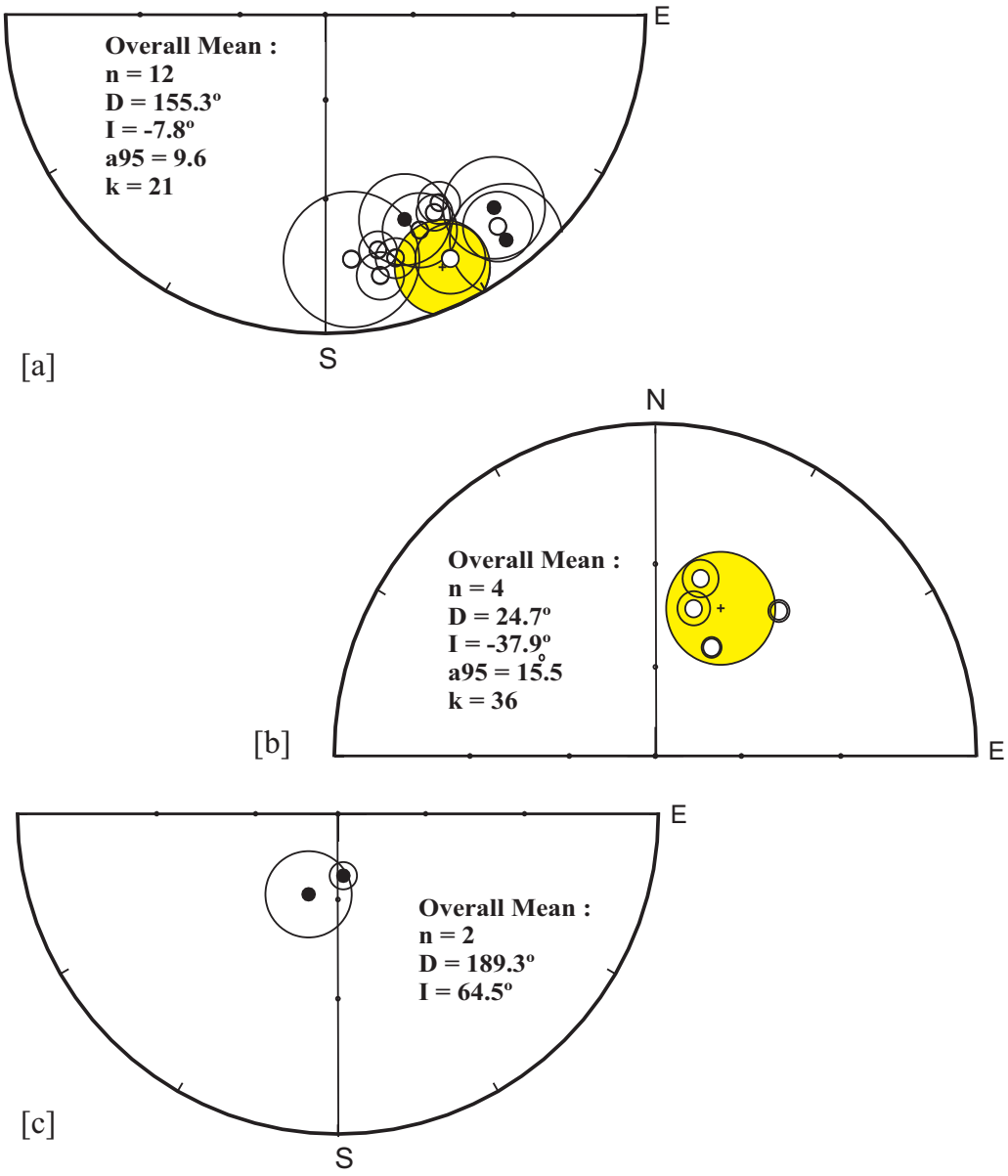

Fig. 9. (a) Stereoplot of site mean directions from the 12 NW–SE trending dykes from the older suite (Dec = 155.3° and Inc = −7.8°). (b) Stereoplot of site mean directions from ENE–WSW Mahoba suite of dykes (Dec = 24.7° and Inc = −37.9°). (c) Stereoplot of site mean directions from NE–SW trending third set of dykes (Dec = 189.3° and Inc = 64.5°) with a palaeolatitude of 46.4°N.

to the inadequate averaging of secular variation (Salminen et al., 2009). Given the tentative nature of the Salla diabase pole, we select the previously reported mean paleomagnetic pole from the Bamble intrusions to place Baltica in our reconstruction (Brown and McEnroe, 2004; Stearn and Piper, 1984).

A key, well-dated paleomagnetic pole, from the Kalahari craton at ~1.1 Ga is based on the Umkondo dolerites and the Kalkpunt poles (Hanson et al., 2004a; Gose et al., 2004, 2006; Jacobs et al., 2008). The precisely dated Umkondo dolerite paleomagnetic data from the Kalahari craton are often correlated with Keweenawan igneous suite of Laurentia (Hanson et al., 2004a; Gose et al., 2006; Jacobs et al., 2008). These two coeval paleomagnetic poles are predominantly of one polarity and thus constrain the relative paleolatitudes of the two cratons within the Rodinia configuration. The paleomagnetic data in our reconstruction at ~1.1 Ga are derived from the mean pole based on the results from Timbavati gabbros, the Umkondo–Borg large igneous province and the Grunehogna province of Antarctica after restoring East Antarctica to its position next to South Africa at ~1.1 Ga (Jones and McElhinny, 1966; Renne et al., 1990; Hargraves et al., 1994; Jones and Powell, 2001; Powell et al., 2001; Pesonen et al., 2003; Hanson et al., 2004a; Gose et al., 2006; Jacobs et al., 2008).

The reconstruction discussed herein also utilizes the mean paleomagnetic pole from the granophyres and rhyolite nunataks of Coats Land, Antarctica to evaluate the paleogeographic position of Coats Land in Rodinia and their connection to the Kalahari craton at ~1.1 Ga (Gose et al., 1997). The granophyres and rhyolite nunataks provide indistinguishable mean paleomagnetic directions with precise U–Pb zircon ages of 1112 ± 4 Ma (rhyolites) and 1106 ± 3 Ma (granophyres) respectively. These volcanic rocks are interpreted to represent part of the Umkondo–Borg–Keweenawan magmatic province (Jacobs et al., 2008).

The position of North China Block in Late Mesoproterozoic times (~1100 Ma) is constrained by paleomagnetic data from the Tieling

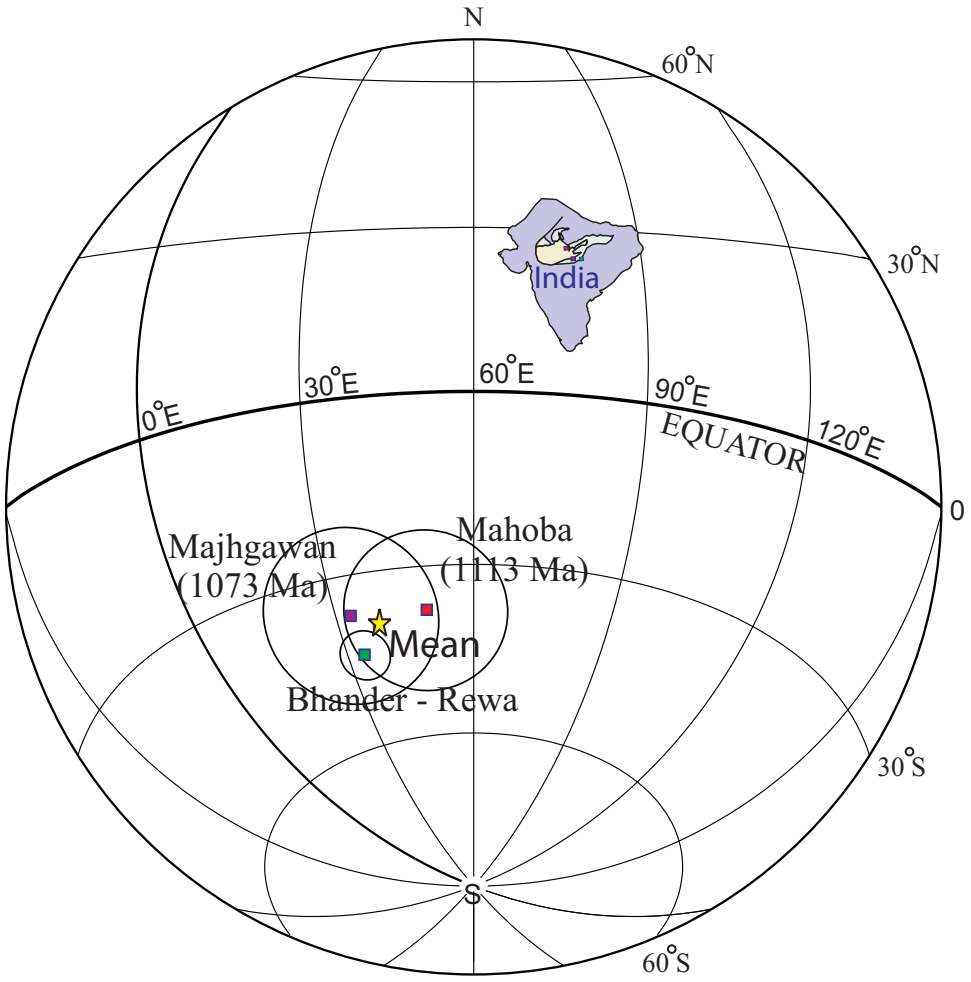

Fig. 10. Schmidt projection of virtual geomagnetic poles (VGP) from the Mahoba dykes (this study) and the Majhgawan kimberlite (Gregory et al., 2006) correlated to the mean paleomagnetic pole of the Bhander–Rewa Groups of the Upper Vindhyan Sequence (Malone et al., 2008). The locations of these sites are shown in the inset map of India (red square: Mahoba dykes; magenta square: Majhgawan kimberlite; and green square: Bhander–Rewa). (For interpretation of the references to color in this figure legend, the reader is referred to the web version of this article.)

formation of the Jixian Province (Zhang et al., 2006). The paleomagnetic pole appears to be primary having passed both fold and reversal tests; however, the age of the magnetization remains tentative. Nevertheless, we use these results to position the North China block in our reconstruction.

The position of the Siberian block is contentious during Rodinia assembly (Sears and Price, 2000; Pisarevsky and Natapov, 2003; Meert and Torsvik, 2003; Li et al., 2008; Pisarevsky et al., 2008). In a majority of Rodinia configurations, Siberia is placed with its (present-day) southern margin in the vicinity of northern Laurentia (Gallet et al., 2000; Pisarevsky and Natapov, 2003; Li et al., 2008). Others argue for either non-inclusion of the Siberian craton within the Rodinia assembly (Meert and Torsvik, 2003; Pisarevsky et al., 2008) or place Siberia adjacent to the present-day Cordilleran margin of Laurentia (Sears and Price, 2003). We use paleomagnetic data from the Late Mesoproterozoic Malgina and Linok formations of southeastern Uchur-Maya region and northeastern Turukhansk region of the Siberia craton (Gallet et al., 2000) in our reconstruction. Chemostratigraphic, biostratigraphic and isotopic data constrain the age of these two formations between 1100 and 1050 Ma and the presence of positive fold and reversal tests; together with a conglomerate test suggest a primary magnetization in these rocks.

Fig. 11 shows the paleogeographic reconstruction of Rodinia at ~1.1 Ma utilizing the paleomagnetic poles from the above mentioned cratonic blocks. This time period of 1100 Ma is known to record the first phase of Rodinia assembly (Pesonen et al., 2003). Our reconstruction is based on the "closest approach" technique as described in Meert and Stuckey (2002); Buchan et al. (2000, 2001) and Pesonen et al. (2003), using individual poles to reconstruct the continents to their correct palaeolatitudinal position since paleomagnetism cannot provide longitudinal control.

In our reconstruction, the combined mean of Portage Lake volcanics and Keweenawan poles (normal + reversed) (Pesonen et al., 2003; Goodge et al., 2008; Swanson-Hysell et al., 2009) places Laurentia at an intermediate latitudinal position with the North China block at its present day north and Australia located further south. Zhang et al. (2006) suggested a common APW path for the North China Block (NCB) and Laurentia from ca. 1200 to ca. 700 Ma in support of an NCB–Laurentia connection during this interval. Siberia is placed at a distance from Laurentia to accommodate the North China block, with its southern margin facing the northern margin of Laurentia (Rainbird et al., 1998; Pisarevsky et al., 2008). While the position of Laurentia is well constrained at this interval, the placement and orientation of Siberia and NCB remains poorly understood and requires additional support. Pesonen et al. (2003) suggested a southerly drift for Baltica away from Laurentia between 1.25 and 1.1 Ga based on the paleomagnetic data from the Sveconorwegian Province (Poorter, 1975; Patchett and Bylund, 1977; Pesonen and Neuvonen, 1981). In our reconstruction, Baltica occupies an

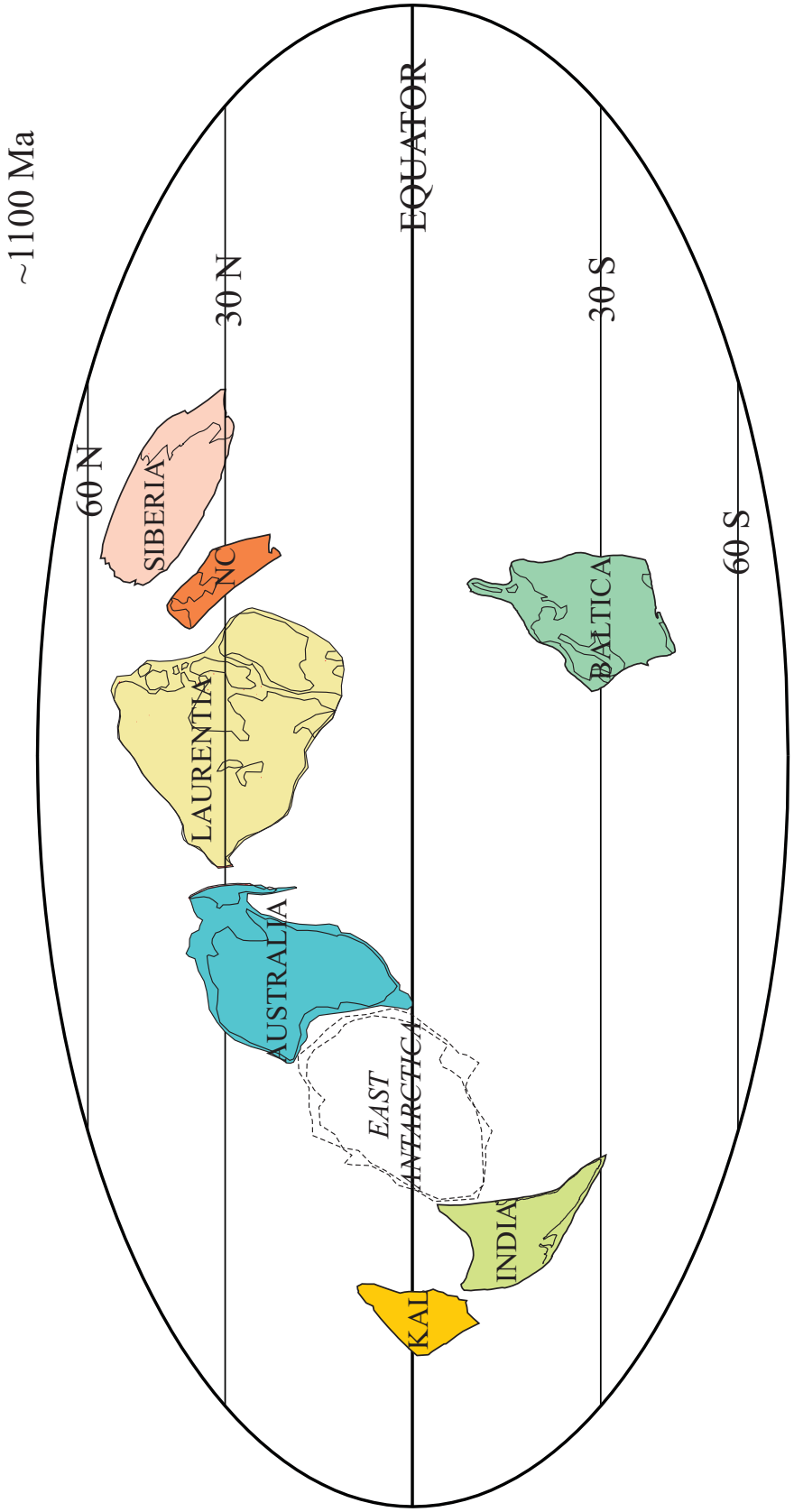

Fig. 11. Paleomagnetically based reconstruction at ~1.1 Ga based on our combined virtual geomagnetic pole (VGP) from ~1113 Ma Mahoba dykes of the Bundelkhand craton (this study); Majhgawan kimberlite pole (~1073 Ma; Gregory et al., 2006) and Bhander–Rewa pole (Malone et al., 2008) and data reported in Pesonen et al. (2003) that places India at low latitudinal position to ~mid latitudinal positions for Australia (Bangemall sill pole) (Paleolongitudes are unconstrained; see Table 3a).

independent southerly latitudinal position derived from the combined paleomagnetic pole from the 1095 Ma Bamble intrusives. A tighter fit can be obtained between the Baltica and Laurentia by inverting the polarity of the Bamble dykes pole; however, this position would require southern Baltica to face the northern margin of Laurentia for which there is little support from the geology. Thus, we follow the southern palaeolatitudinal option of Pesonen et al. (2003) to constrain Baltica in our reconstruction (also see Salminen et al., 2009).

Based on the available paleomagnetic data from Kalahari and Laurentia, Kalahari is located too far south of Laurentia to support any linkage between the two blocks (Hanson et al., 2004a; Gose et al., 2006). The ~1070 Ma Bangemall Sill pole from Western Australia (Wingate et al., 2002) constrains the Australia–Mawson landmass at low to intermediate palaeolatitudes along the southern margin of Laurentia. In their reconstruction, Powell and Pisarevsky (2002) suggested that the Kalahari craton is separated from Laurentia by the Australia–Mawson cratons. They noted that ~1080 Ma deformation in the Darling belt along the western margin of Australian margin might link with the coeval deformation in the Natal and Maud belts along the southern margin of Kalahari. Such an interpretation is possible within the framework of Fig. 11. This separation of the Kalahari and Laurentia at 1.1–1.0 Ga is such that it allows the placement of parts of East Gondwana to the southwest or south of Laurentia (Meert and Torsvik, 2003; Pesonen et al., 2003). Among the elements of the East Gondwana, the link between India and East Antarctica remains paleomagnetically untested for this interval due to the absence of any paleomagnetic data from East Antarctica at ~1100 Ma. However, the proposed geological coherence of the Mawson block with Australia in post-1200 Ma Rodinia reconstructions (Cawood and Korsch, 2008; Payne et al., 2009; Wang et al., 2008; Kelly et al., 2002; Torsvik et al., 2001) and the disposition of India at low latitudes (this study) do favor a loose association of these cratonic elements, with India positioned at the southern margin of the Mawson block. Meert et al. (1995) and Meert (2003) argue that East Gondwanaland was not a coherent entity until late Neoproterozoic or Early Cambrian (see also Fitzsimons, 2000a,b; Boger et al., 2001, 2000; Powell and Pisarevsky, 2002). We have reliable paleomagnetic data from India and Australia, but to make any robust conclusion our interpretation relies upon additional paleomagnetic data from the East Antarctica craton at this interval.

The time period of ~1.1 Ga represents the initial phase of the Rodinia amalgamation. Our paleomagnetic reconstruction at ~1.1 Ga is based on the existing database with smaller number of continental blocks well constrained in space and time. The palaeoconfiguration of these blocks suggest a loose association within Rodinia with no paleomagnetic poles from majority of the West Gondwana elements.

5.2. ~2.0 Ga paleomagnetism

5.2.1. Tectonic evolution of the Aravalli and Dharwar protocontinents

A series of collisional events took place during the Paleoproterozoic interval (~2.1–1.8 Ga) on a near global scale (Zhao et al., 2002; French et al., 2008). The 2.0–1.8 Ga orogenic belts are thought to be the result of accretion of Archaean cratonic nuclei to form numerous supercratons or possibly, a supercontinent (Hoffman, 1988; Gower et al., 1990, 1992; Krapez, 1999; Rogers and Santosh, 2002, 2003; Condie, 2002; Zhao et al., 2002, 2004a,b).

The Central Indian Tectonic zone (CITZ) is a linear Paleoproterozoic orogenic belt that represents the locus of collision between the northern Aravalli protocontinent (Aravalli-Delhi belt, Bundelkhand massif and Vindhyan basin) and the southern Dharwar protocontinent (Bastar, Singhbhum, Dharwar cratons and Southern Indian Granulite terrane; Fig. 12a). The connection between the Bastar, Singhbhum and Dharwar cratons of the South Indian block is well established at least by 1.9 Ga (Ramchandra et al., 1995; French et al., 2008). The temporal control on the collision between the Aravalli and the Dharwar protocontinents is still contentious (Meert et al., 2010). Stein et al. (2004) proposed an oblique collision between the northern and southern blocks around 2.5 Ga with the initiation of the formation of CITZ at this time. Other authors argue for an ~1.9 to 1.6 Ga collision between the two blocks (Acharyya, 2003) or even much younger ~1.0 Ga (Bhowmik et al., 2011).

If we accept a pre-2.0 Ga age for the amalgamation between the northern and southern Indian cratons, then we can use our new paleomagnetic data from the ~2.0 Ga NW–SE trending mafic dykes intruding the Bundelkhand craton combined with paleomagnetic data from the ~1.9 Ga mafic dykes of the Bastar craton (Meert et al., 2010; French et al., 2008), Cuddapah trap volcanics (Clark, 1982) and a dyke adjacent to the Cuddapah basin in the Dharwar craton (Kumar and Bhalla, 1983) to provide some insight into the drift history of the Aravalli and Dharwar protocontinents (Fig. 12b). The combined result from the ~2.0 Ga NW–SE trending older suite of dykes from the Bundelkhand craton yield a paleomagnetic pole for India at 58.5°N and 312.5°E ($dp = 4.9°$; $dm = 9.7°$) and places the Bundelkhand craton in an equatorial position (Fig. 12b). The combined 1.9 Ga paleomagnetic pole for the Dharwar and Bastar cratons falls at 31° N, 330°E ($dp = 6.3°$; $dm = 12.2°$) and also places these cratonic nuclei at low latitudes (Meert et al., 2011). A nearly equatorial position for the Bundelkhand craton is also indicated by the paleomagnetic data from ~1.8 Ga Gwalior volcanics of the Bundelkhand craton that generates a paleomagnetic pole for the cratonic nuclei at 15.4°S and 353.2°E ($dp = 5.6$; $dm = 11.2$; Pradhan et al., 2010). Utilizing the three paleomagnetic poles from the Bundelkhand dykes, Bastar–Cuddapah dykes and the Gwalior volcanics, an apparent polar wander (APW) path was constructed for the Indian peninsular shield during the 2.0–1.8 Ga interval (Fig. 12b). The APWP indicates that India rotated through 80 degrees with only slight changes in paleolatitude during this interval.

5.2.2. Implications for Columbia

The Paleo–Mesoproterozoic history of the Earth is punctuated by the presence of globally distributed 2.1–1.8 Ga collisional orogens related to a proposed pre-Rodinian supercontinent named Columbia (Zhao et al., 2002, 2004a,b; Condie, 2000, 2002; Rogers and Santosh, 2002; Kusky et al., 2007; French and Heaman, 2010). In particular, the Columbia model by Zhao et al. (2004a,b) is based primarily on the geological connections between globally distributed cratonic nuclei and the presence of the Paleo–Mesoproterozoic orogenic belts (2.1–1.8 Ga; Fig. 13a).

Reliable paleomagnetic data provide a quantitative reference frame for documenting the history and dynamics of the plate tectonic regime and constraining the position of various cratonic blocks within the proposed continental assemblies. Any attempt at global reconstructions in the Precambrian is an arduous task due to the scarcity of well-dated paleomagnetic data, polarity ambiguity and the absence of longitudinal control in positioning of the continents (Van der Voo and Meert, 1991; Meert, 2002; Meert et al., 2011). In addition, the majority of present day continents are an amalgam of older Archean cratonic nuclei that were not fully welded until Mesoproterozoic or later time.

The paleomagnetic database for the Paleoproterozoic has improved over the past decade as reliable and well-dated poles are becoming more commonplace. Below, we discuss the paleogeographic reconstruction of the Paleoproterozoic Columbia supercontinent utilizing the most updated paleomagnetic results from various cratonic blocks at ~2.0 Ga (Fig. 13b; Table 3a).

The ~2.0 Ga paleomagnetic pole calculated from the NW–SE trending dyke suite of the Bundelkhand craton constrains the

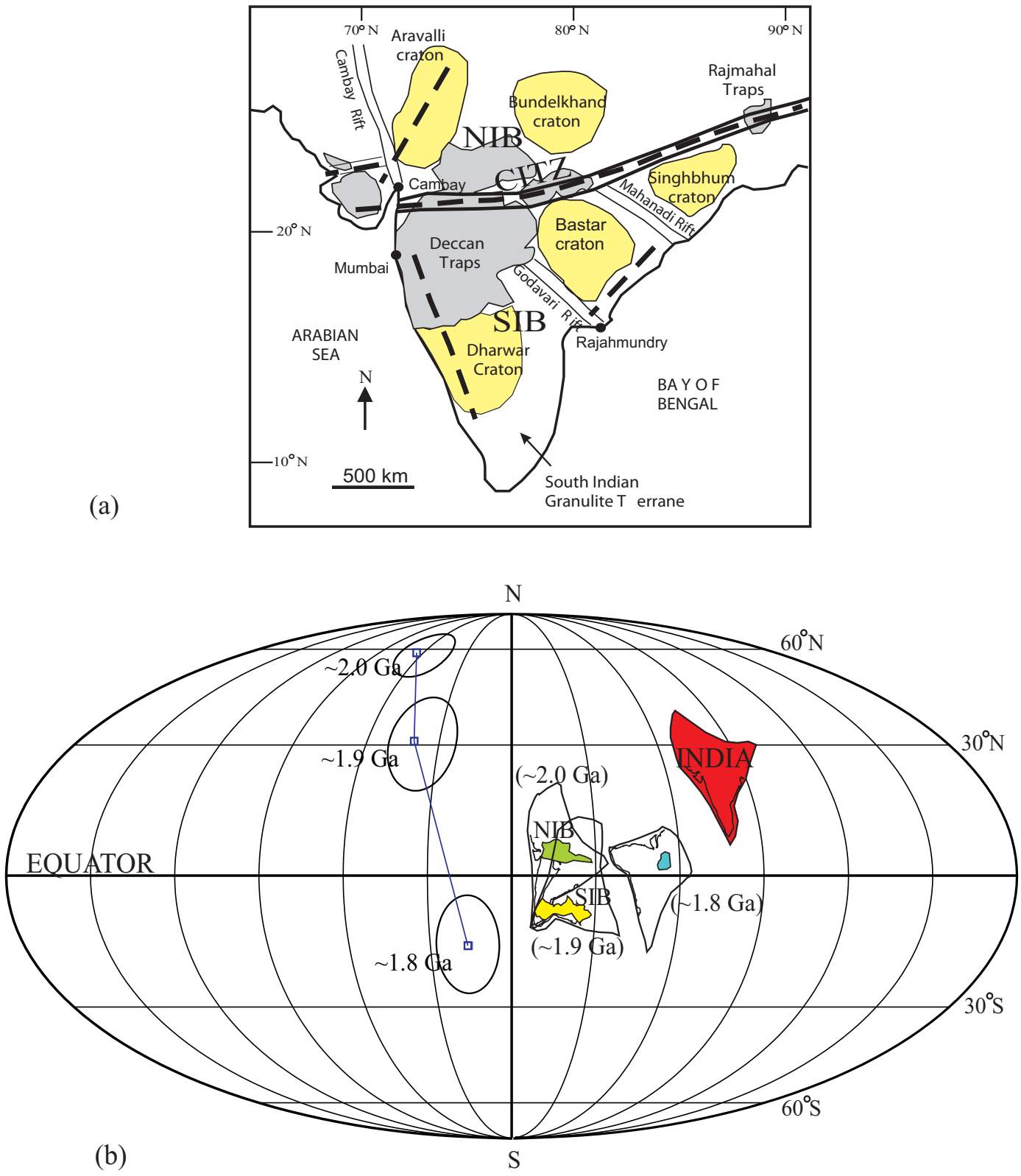

Fig. 12. (a) Generalized tectonic map of India showing the North Indian Block (Aravalli protocontinent) and South Indian Block (Dharwar protocontinent) docked together along Central Indian Tectonic Zone (CITZ). (b) Positions of northern Aravalli-Bundelkhand protocontinent (~2.0 Ga) and southern Dharwar protocontinent (~1.9 Ga) of the Indian peninsular shield based on the paleomagnetic poles from the ~2.0 Ga NW–SE trending Bundelkhand dyke suite, ~1.9 Ma Bastar dykes/Cuddapah dykes of the Bastar/Dharwar cratons and ~1.8 Ga Gwalior volcanics. The figure also shows the APW path for India utilizing the paleopoles from ~2.0 to 1.8 Ga.

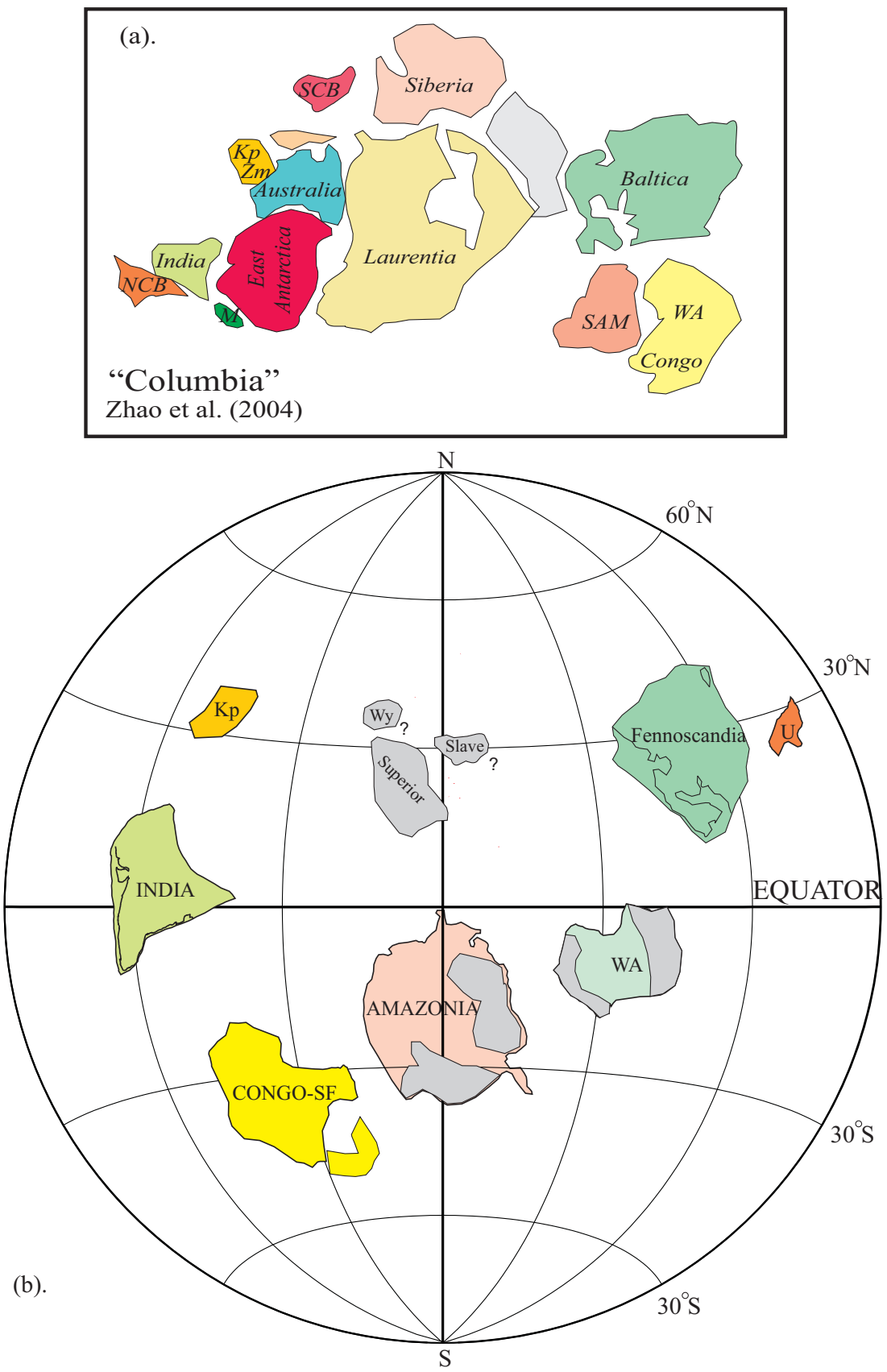

Fig. 13. Paleomagnetically based reconstruction at ~2.0 Ga (after Pesonen et al., 2003). The Bundelkhand craton is positioned according to paleomagnetic data from the ~1980 Ma NW–SE trending dykes reported in this paper. The reconstruction places India at the equatorial positions with mid latitudinally located Laurentia (Sl: Slave and Wy: Wyoming cratons). The other continental blocks used in the reconstruction are Amazonia, Congo-SF, Kp: Kaapvaal, Fennoscandia, Ukraine, WA: West Africa (Palaeolongitudes are unconstrained; see Table 3b).

Table 3a
Paleomagnetic poles at ca. ~1.1 Ga.

Continent	Pole name	Age	Plat	Plong	A95	Reference
India	Mahoba dykes	1113 ± 7 Ma	37.8°S	49.5°E	15.5°	This study
Laurentia	Keweenawan dykes mean + Portage volcanic	1090 Ma	36°N	188°E	3°	Swanson-Hysell et al. (2009), Pesonen et al. (2003)
Baltica	Mean Baltica	1093 Ma	1°N	208°E	16°	Pesonen et al. (2003)
Australia	Bangemall sill pole	1070 Ma	83.7°S	129°E	8.3°	Wingate et al. (2002)
Kalahari	Mean Kalahari	1096 Ma	65°S	225°E	5°	Gose et al. (2006), Pesonen et al. (2003)
Siberia	Malgina + linok formation	1078 Ma	25°S	231°E	3°	Gallet et al. (2000)

Table 3b
Paleomagnetic poles at ca. ~2.0 Ga.

Continent	Pole name	Age	Plat	Plong	A95	Reference
India	NW–SE Bundelkhand dykes	1980 ± 9 Ma	58.5°N	312.5°E	9.6°	This study
Superior craton (Laurentia)	Minto Dykes	1998 ± 2 Ma	38°N	174°E	10.0°	Buchan et al. (1998)
Fennoscandia	Konchozero sill, Karelia	1974 ± 27 Ma	14.2°S	282°E	11.0°	Pisarevsky and Sokolov (1999)
Ukraine	Gabbro Monzonite + Gabbro diabase	2000 Ma	53°N	142°E	–	Pesonen et al. (2003), Elming and Mattsson (2001)
Amazonia	Oyapok tonalites + Encrucijada pluton	2019 Ma	42°N	181°E	4.0°	Pesonen et al. (2003)
Congo-SF	Uauá dykes	1983 ± 31 Ma	24°N	331°E	4.0°	D'Agrella-Filho and Pacca (1998)
Kalahari	Vredefort dykes	2023 Ma	27°N	31°E	7.0°	Salminen et al. (2009), Pesonen et al. (2002)
West-Africa	Liberia M	2050 ± 6 Ma	18°S	89°E	13.0°	Onstott and Dorbor (1987)

position of the North Indian Block (Aravalli protocontinent) in our reconstruction. As noted above, the North Indian and the South Indian blocks of the peninsular India were in close proximity during 2.1–1.9 Ga (also see Meert et al., 2011; Stein et al., 2004). Hence, we suggest that the ~2.0 Ga pole from the Bundelkhand dykes is representative of a major portion of Peninsular India for this time period (Table 3b).

The palaeolatitudinal position of the Superior craton of the Laurentian block is constrained at ~2.0 Ga via the paleomagnetic data from the diabase dykes of the Minto block of the northeastern Superior Province (Buchan et al., 2000). The Minto dykes paleomagnetic pole has a positive baked contact test and is precisely dated at 1998 ± 2 Ma by U–Pb isotopic methods (Buchan et al., 2000). Most of the other cratonic nuclei of Laurentia such as Slave–Rae–Hearne and Wyoming blocks collided with the Superior craton during Trans-Hudson orogeny (2.1–1.8 Ga), although the terminal collision was protracted until ~1.78 Ma (Corrigan et al., 2005). Recent paleomagnetic studies on the Lac de Gras diabase dykes across the Slave Province of the Canadian Shield suggest that the Slave and Superior cratons were located at similar latitudes at ~2.02 Ga but with different relative orientations than today (Buchan et al., 2009). Due to the absence of coeval paleomagnetic data from other cratonic blocks of Laurentia at ~2.0 Ga, we use the Minto dyke pole as representative for Laurentia assuming that the other Laurentian nuclei were in close proximity during this period.

A low to intermediate latitudinal position for the Fennoscandian shield during Paleoproterozoic is based on paleomagnetic data between 2.2 and 1.97 Ga (Pisarevsky and Sokolov, 1999; Neuvonen et al., 1997; Mertanen and Pesonen, 1994). The paleoposition of the Fennoscandia is constrained in our reconstruction utilizing the only available paleomagnetic pole from the 1974 ± 27 Ma (Sm–Nd age) Konchozero peridotite sill (component I) of the Fennoscandia (Pisarevsky and Sokolov, 1999).

According to Bogdanova et al. (1994) the Ukranian shield was probably attached to the Fennoscandia at ca. 2.0 Ga. However, the paleomagnetic data for the Ukranian shield between ca. 2.0 and 1.72 Ga suggest that the final accretion of Fennoscandia to the Ukranian shield took place sometimes after ca. 1.8 Ga (Elming and Mattsson, 2001). The position of the Ukranian shield at ~2.0 Ga in our reconstruction is derived from the paleomagnetic data from the gabbro diabase dyke of the southern Sarmatia province of Baltica (Elming and Mattsson, 2001).

The Kalahari craton of South Africa consists of the Kaapvaal and the Zimbabwe blocks welded together along the Limpopo belt sometime between 1.9 and 2.06 Ga (De Wit et al., 1992; Lubnina et al., 2010; Hanson et al., 2011). Paleomagnetic data for the Zimbabwe craton at ~2.0 Ga are lacking and therefore its connection with the Bushveld complex of the Kaapvaal craton is also ambiguous (Lubnina et al., 2010; Söderlund et al., 2010). We use updated paleomagnetic data from the ~2.02 Ga Vredefort dykes/impact structures of the Kaapvaal craton to constrain its position at ~2.0 Ga in our reconstruction (Salminen et al., 2009; Carporzen et al., 2006; Pesonen et al., 2002).

The metamorphosed Uauã mafic dykes of São Fransisco provide the only paleomagnetic pole for Congo-São Fransisco cratons at ~2.0 Ga (D'Agrella-Filho and Pacca, 1998). Paleomagnetic, petrographic and geochronological evidence support a secondary origin of magnetization in these dykes, probably acquired approximately at 2–1.9 Ga, during the uplift and regional cooling of the Transamazonian cycle (D'Agrella-Filho and Pacca, 1998).

Nomade et al. (2003, 2001) reported a paleomagnetic pole from the Oyapok–Campoi river zone (OYA in their manuscript) of the French Guiana shield of the Amazonian craton with a magnetization age of 2036 Ma. Other paleomagnetic poles that exist for the Amazonian craton at ~2.0 Ga come from the Encrucijada pluton of the Venezuela block (Onstott and Hargraves, 1981). The statistical precision on the Rb–Sr ages of the Encrucijada granites are poor and the ages are considered rather inconsistent. The two poles are significantly different and, on the basis of the difference, it was argued that there was northward movement along the Pisco Jurua fault zone during the 2036–2000 Ma period (Onstott and Hargraves, 1981; Nomade et al., 2001). Although not united but lying in close association, we consider the OYA poles to constrain the position of the Amazonia craton in our ~2.0 Ga reconstruction.

Utilizing all the available paleomagnetic data from the cratonic blocks mentioned above, we attempt to test the proposed Columbia configuration of Zhao et al. (2002, 2004a,b). Fig. 13a represents the typical Columbia configuration of Zhao et al. (2004a,b) based on the correlation of the coeval orogenic belts (2.1–1.8 Ga) within its

constituent cratonic blocks. Zhao et al. (2004a,b) configuration is not supported by the existing paleomagnetic database at ca. 2.0 Ga (Fig. 13b; Table 3a). The majority of these continental nuclei occupy low to intermediate latitudinal positions as they did in the Kenorland assembly at ca. 2.45 Ga (Salminen et al., 2009; Pesonen et al., 2003). The only resemblance to the Columbia model by Zhao et al. (2004a,b) is exhibited by the juxtaposition of the parts of Amazonia and West-Africa (Fig. 13b; Table 3a).

In the traditional Columbia configuration, India is placed adjacent to East Antarctica and North China along the present day south-western margin of Laurentia (Zhao et al., 2004a,b). The Kalahari craton of South Africa, on the other hand, is positioned along the north-western margin of Australia (Fig. 12a). In our reconstruction, the new paleomagnetic data from ~2.0 Ga Bundelkhand dykes (this study) constrain the position of India at nearly equatorial latitudes with Laurentia occupying low to intermediate latitudes. The Kaapvaal block of the Kalahari craton can be placed at mid-latitudes either north or south depending upon polarity choice. Baltica did not exist as a coherent block at ~2.0 Ga and the available paleomagnetic data from the Fennoscandian and the Ukrainian shield position these two blocks at mid-latitudes with no obvious connection to Laurentia (Salminen et al., 2009).

The African and South-American continental fragments represent a loose connection in the configuration at ~2.0 Ga and may show the only resemblance to the archetypal Columbia model of Zhao et al. (2004a,b). The low southerly latitudinal positions indicated by the paleomagnetic data for Amazonia, West Africa and Congo–Sao Fransisco blocks may indicate that these were juxtaposed at ~2.0 Ga (Nomade et al., 2001, 2003). The presence of coeval Trans-Amazonian and Eburnean orogenic events in Amazonia (Hartmann, 2002) and West Africa (Ledru et al., 1994) respectively, may lend additional support to their connection at 2.1–1.9 Ga.

Although our reconstruction at ~2.0 Ga is based on limited number of paleomagnetic poles from a small number of cratonic blocks, most of the poles are reasonably constrained in both time and space. Thus, we cannot reject the existence of a "Columbia-type" supercontinent during the Paleoproterozoic; though the independent drift of most of the continental blocks at ~2.0 Ga enables us to reject some of the relationships between cratonic blocks suggested in the Columbia model by Zhao et al. (2004a,b).

6. Conclusions

(1) The paleomagnetic and geochronological results on the mafic dyke swarms intruding the Archean–Paleoproterozoic Bundelkhand craton presented in this paper are significant not only in providing reliable age constraints for these magmatic events, but also for improving our understanding of the tectonic evolution of the Central Indian shield. The three distinctive paleomagnetic directions obtained in this study for the mafic dyke swarms suggest three different pulses of emplacement within the BC. The precise U–Pb isotopic zircon age of ~1980 Ma for the NW–SE trending dyke (sample I9GS-13) and 1113 Ma for the ESE–WSW trending great dyke of Mahoba support our paleomagnetic analysis and the geologic correlations.

(2) This study provides a refined virtual geomagnetic pole for the Mahoba suite of dykes at 37.8°S, 49.5°E ($dp/dm = 10.8/18.3$). This geomagnetic pole correlates well with the VGP generated for the Majhgawan kimberlite and the poles from the Bhander–Rewa Groups of the Upper Vindhyan sequence (Gregory et al., 2006; Malone et al., 2008). Our interpretation of the Mahoba paleomagnetic and geochronological results lend further support to the argument that the closure age for the Upper Vindhyan rocks is older than 1000 Ma.

(3) The paleomagnetic results from the ~1980 Ma NW–SE trending dyke suite of the Bundelkhand craton along with other published data from 1800 to 2000 Ma interval indicates a close proximity between the major elements of Peninsular India (Aravalli-Bundelkhand and Dharwar-Bastar and Singhbhum cratons). This would suggest that the younger tectono-magmatic events recorded in the CITZ represent crustal-scale reactivation along an existing zone of weakness.

(4) We also provide paleogeographic reconstructions at 2.0 and 1.1 Ga. Our ~2.0 Ga pole from the NW–SE trending Bundelkhand dykes favors a low latitudinal position for India with mid latitudinal disposition of Laurentia and the Kaapvaal block. The proposed connection of India to East Antarctica and North China (Zhao et al., 2004a,b) remains untested due to the absence of paleomagnetic data from North China and East Antarctica cratons at ~2.0 Ga. Laurentia and India can be placed in proximity to each other but in a vastly different configuration than that suggested by Zhao et al. (2004a,b) based on the geometric relationships of the radiating dyke swarms. The global paleogeography at ~2.0 Ga favors scattered independent continental blocks as suggested by Pesonen et al. (2003; also see Salminen et al., 2009) and does not support the Columbia model of Zhao et al. (2004a,b).

(5) With reference to Rodinia, one of the interesting implications of our results from ~1113 Ma Mahoba dyke pole in conjunction with the coeval Majhgawan kimberlite and Bhander–Rewa poles is that it infers a low latitudinal position for India with Australia–Mawson blocks located at mid latitudes. The link between India and East Antarctica remains paleomagnetically untested for this interval due to the absence of any paleomagnetic data from the East Antarctica block. However, the proposed geological coherence of the Mawson block with Australia in post-1200 Ma configurations (Cawood and Korsch, 2008; Payne et al., 2009; Wang et al., 2008; Kelly et al., 2002; Torsvik et al., 2001) and the disposition of India at low latitudes (this study) might indicate a loose East Gondwana fit, with India positioned further south of East Antarctica.

Acknowledgements

This work was supported by a grant from the US National Science Foundation to J.G. Meert (EAR09-10888). We wish to thank Shawn Malone for the careful proofreading of the manuscript. We would also like to thank Dr. Rajesh Srivastava and an anonymous reviewer for the thorough and thoughtful review of the manuscript.

References

Acharyya, S.K., 2003. The nature of the Mesoproterozoic Central Indian Tectonic Zone with exhumed and reworked older granites. Gondwana Research 6, 197–214.
Auden, J.B., 1933. Vindhyan sedimentation in the Son-Valley, Mirzapur district. Memoir of Geological Survey of India, 141–250.
Azmi, R.J., Joshi, D., Tiwari, B.N., Joshi, M.N., Srivastava, S.S., 2008. A synoptic view on the current discordant geo- and biochronological ages of the Vindhyan Supergroup, Central India. Himalayan Geology 29, 177–191.
Basu, A.K., 1986. Geology of parts of Bundelkhand and Granite Massif Central India. Geological Survey of India Records 117, 61–124.
Bleeker, W., Ernst, R.E., 2006. Short-lived mantle generated magmatic events and their dyke swarms: the key to unlocking Earth's paleogeographic record back to 2.5 Ga. In: Symposium Volume for Fifth International Dyke Conference, Balkema, Rotterdam, July–August 2005.
Bhowmik, S.K., Wilde, S.A., Bhandari, A., Pal, T., Pant, N.C., 2011. Growth of the Greater Indian landmass and its assembly in Rodinia: geochronological evidence from the Central Indian Tectonic Zone. Gondwana Research, doi:10.1016/j.gr.2011.09.008.
Boger, S.D., Carson, C.J., Wilson, C.J.L., Fanning, C.M., 2000. Neoproterozoic deformation in the Radok Lake region of the northern Prince Charles Mountains East Antarctica; evidence for a single protracted orogenic event. Precambrian Research 104, 1–24.

Boger, S.D., Wilson, C.J.L., Fanning, C.M., 2001. Early Paleozoic tectonism with the East Antarctic craton: the final suture between east and west Gondwana. Geology 29, 463–466.
Bogdanova, S.V., Bibikova, E.V., Gorbachev, R., 1994. Palaeoproterozoic U–Pb zircon ages from Belorussia: new geodynamic implications for the East European craton. Precambrian Research 68, 231–240.
Buchan, K.L., Mertanen, S., Park, R.G., Pesonen, L.J., Elming, S.-Å., Abrahamsen, N., Bylund, G., 2000. Comparing the drift of Laurentia and Baltica in the Proterozoic: the importance of key poles. Tectonophysics 319, 167–198.
Buchan, K.L., Ernst, R.E., Hamilton, M.A., Mertanen, S., Pesonen, L.J., Elming, S.A., 2001. Rodinia: the evidence from integrated palaeomagnetism and U–Pb geochronology. Precambrian Research 110, 9–32.
Buchan, K.L., LeCheminant, A.N., Breemen, O.V., 2009. Paleomagnetism and geochronology of Lac de Gras diabase dyke swarm, Slave Province, Canada: implications for relative drift of Slave and Superior provinces in the Paleoproterozoic. Canadian Journal of Earth Sciences 46, 361–379.
Burke, K., Dewey, J.F., 1972. Orogeny in Africa, in Dessauvagie. In: Whiteman, T.F.W.A.J (Ed.), Proceedings of the Ibadan Conference on African Geology. Ibadan, Nigeria, December, 1970, pp. 583–608.
Brown, L.L., McEnroe, S.A., 2004. Palaeomagnetism of the Egersund–Ogna anorthosite, Rogaland, Norway, and the position of Fennoscandia in the Late Proterozoic. Geophysical Journal International 158, 479–488.
Cawood, P.A., Korsch, R.J., 2008. Assembling Australia: Proterozoic building of Australia. Precambrian Research 166, 1–38.
Carporzen, L., Gilder, S.A., Hart, R.J., 2006. Origin and implications of Verwey transitions in the basement rocks of the Vredefort meteorite crater, South Africa. Earth and Planetary Science Letters 251, 305–317.
Chakrabarti, A., 1990. Traces and dubiotraces: examples from the so called Late Proterozoic silisiclastic rocks of the Vindhyan SuperGroup around Maihar, India. Precambrian Research 47, 141–153.
Clark, D.A., 1982. Preliminary paleomagnetic results from the Cuddapah traps of Andhra Pradesh. Monograph-2, On Evolution of the intracratonic Cuddapah Basin, HPG, Hyderabad, India, pp. 47–51.
Condie, K.C., 2002. Breakup of a Paleopreoterozoic supercontinent. Gondwana Research 5, 41–43.
Corrigan, D., Hajnal, Z., Nemeth, B., Lucas, S.B., 2005. Tectonic framework of a Palaeoproterozoic arc-continent to continent-continent collisional zone, Trans-Hudson Orogen, from geological and seismic reflection studies. Canadian Journal of Earth Sciences 42, 421–434.
Crawford, A.R., 1975. The Precambrian geochronology of Rajasthan and Bundelkhand, northern India. Canadian Journal of Earth Sciences 7, 91–110.
Crawford, A.R., Compston, W., 1970. The age of Vindhyan system of peninsular India. Quaternary Journal of Geological Society of London 125, 351–371.
Dalziel, I.W.D., 1991. Pacific margins of Laurentia and East Antarctica–Australia as a conjugate rift pair: evidence and implications for an Eocambrian supercontinent. Geology 19, 598–601.
Dalziel, I.W.D., 1997. Neoproterozoic–Paleozoic geography and tectonics: review, hypothesis and environmental speculation. Bulletin of the Geological Society of America 109, 16–42.
Dalziel, I.W.D., Mosher, S., Gahagan, L.M., 2000. Laurentia–Kalahari collision and the assembly of Rodinia. Journal of Geology 108, 499–513.
D'Agrella-Filho, M.S., Pacca, I.G., 1998. Paleomagnetism of Paleoproterozoic mafic dyke swarm from the Uauá region, Northeastern São Francisco Craton, Brazil: tectonic implications. Journal of South American Earth Sciences 11, 23–33.
Davis, D., Sutcliffe, R., 1985. U–Pb ages from the Nipigon plate and northern Lake Superior. Geological Society of America Bulletin 96, 1572–1579.
De, C., 2003. Possible organisms similar to Ediacaran forms of the Bhander Group, Vindhyan Super Group, Late Neoproterozoic of India. Journal of Asian Earth Sciences 21, 387–395.
De, C., 2006. Ediacara fossil assemblage in the Upper Vindhyans of Central India and its significance. Journal of Asian Earth Sciences 27, 660–683.
Devaraju, T.C., Laajoki, L., Zozulya, D., Khanadali, S.D., Ugarkar, A.G., 1995. Neo-Proterozoic dyke swarms of southern Karnataka. Part II: geochemistry, oxygen isotope composition, Rb–Sr age and petrogenesis. Memoir Geological Society of India 33, 267–306.
Dewey, J.F., Burke, K.C.A., 1973. Tibetan, Variscan and Precambrian basement reactivation: products of continental collision. Journal of Geology 81, 683–692.
De Wit, M.J., de Ronde, C.E.J., Tredoux, M., Roering, C., Hart, R.J., Armstrong, R.A., Green, R.W.E., Peberdy, E., Hart, R.A., 1992. Formation of an Archean continent. Nature 357, 553–562.
Drury, S.A., 1984. A Proterozoic intracratonic basin, dyke swarms and thermal evolution in south India. Journal of Geological Society of India 25, 437–444.
Elming, S.-Å., Mattsson, H., 2001. Post Jotnian basic intrusion in the Fennoscandian Shield, and the breakup of Baltcia from Laurentia: a palaeomagnetic and AMS study. Precambrian Research 108, 215–236.
Ernst, R.E., Srivastava, R.K., 2008. India's place in the Proterozoic world: constraints from the large igneous provinces (LIP) record. In: Srivastava, R.K., Sivaji, Ch., Chalapathi Rao, N.V. (Eds.), Indian Dykes: Geochemistry, Geophysics, and Geochronology. Narosa Publishing House Pvt. Ltd., New Delhi, India, pp. 41–56.
Ernst, R.E., Wingate, M.T.D., Buchan, K.L., Li, Z.X., 2008. Global record of 1600–700 Ma large igneous provinces (LIPs): implications for the reconstruction of the proposed Nuna (Columbia) and Rodinia supercontinents. Precambrian Research 160, 159–178.
Ernst, R.E., Bleeker, W., 2010. Large igneous provinces (LIPs), giant dyke swarms, and mantle plumes: significance for breakup events within Canada from 2.5 Ga to the present. Canadian Journal of Earth Sciences 47, 695–739, doi:10.1139/E10-025.
Fitzsimons, I.C.W., 2000a. A review of tectonic events in the East Antarctic shield, and their implications for Gondwana and earlier supercontinents. Journal of African Earth Sciences 31, 3–23.
Fitzsimons, I.C.W., 2000b. Grenville-age basement provinces in East Antarctica: evidence for three separate collisional orogens. Geology 28, 879–882.
French, J.E., 2007. U–Pb Dating of Paleoproterozoic mafic dyke swarms of the South Indian shield: implications for paleocontinental reconstructions and identifying ancient mantle plume events. PhD Thesis. University of Alberta, Edmonton, Alberta, 373.
French, J.E., Heaman, L.M., Chacko, T., Srivastava, R.K., 2008. 1891–1883 a southern Bastar craton-Cuddapah mafic igneous events, India: a newly recognized large igneous province. Precambrian Research 160, 308–322.
French, J.E., Heaman, L.M., 2010. Precise U–Pb dating of Paleoprotoerozoic mafic dyke swarms of the Dharwar craton, India: implications for the existence of the Neoarchean supercraton Sclavia. Precambrian Research 183, 416–441.
Gallet, Y., Pavlov, V.E., Semikhatov, M.A., Petrov, P.Y., 2000. Late Mesoproterozoic magnetostratigraphic results from Siberia: paleogeographic implications and magnetic field behavior. Journal of Geophysical Research 105, 16481–16500.
Gopalan, K., MacDougall, J.D., Roy, A.B., Murali, A.K., 1990. Sm–Nd evidence for 3.3 Ga old rocks in Rajasthan, northwestern India. Precambrian Research 48, 287–297.
Goodge, J.W., Vervoort, J.D., Fanning, C.M., Brecke, D.M., Farmer, G.L., Williams, I.S., Myrow, P.M., DePaolo, D.J., 2008. A positive test of east Antarctica–Laurentia juxtaposition within the Rodinia Supercontinent. Science 321, 235–240.
Goodwin, A.M., 1991. Precambrian Geology: The Dynamic Evolution of the Continental Crust. Academic Press, London, p. 666.
Gose, W.A., Helper, M.A., Connelly, J.N., Hutson, F.E., Dalziel, I.W.D., 1997. Paleomagnetic data and U–Pb isotopic age determinations from Coats Land, Antarctica: implications for late Proterozoic plate reconstructions. Journal of Geophysical Research 102, 7887–7902.
Gose, W.A., Johnston, S.T., Thomas, R.J., 2004. Age of magnetization of Mesoproterozoic rocks from the Natal sector of the Namaqua–Natal belt, South Africa. Journal of African Earth Sciences 40, 137–145.
Gose, W.A., Hanson, R.E., Dalziel, I.W.D., Pancake, J.A., Seidel, E.K., 2006. Paleomagnetism of the 1.1 Ga Umkondo large igneous province in southern Africa. Journal of Geophysical Research 111, B09101, doi:10.1029/2005JB003897.
Gower, C.F., Ryan, A.B., Rivers, T., 1990. Mid-Proterozoic Laurentia–Baltica: an overview of its geological evolution and summary of the contributions by this volume. In: Gower, C.F., Ryan, A.B., Rivers, T. (Eds.), Mid-Proterozoic Laurentia–Baltica, vol. 38. Geological Association of Canada, pp. 1–20 (special paper).
Gower, C.F., Schärer, U., Heaman, L.M., 1992. The Labradorian Orogeny in the Grenville Province, eastern Labrador. Canadian Journal of Earth Sciences 29, 1944–1957.
Gregory, L.C., Meert, J.G., Pradhan, V., Pandit, M.K., Tamrat, E., Malone, S.J., 2006. A paleomagnetic and geochronological study of the Majhgawan Kimberlite, India: implications for the age of the Vindhyan SuperGroup. Precambrian Research 149, 65–75.
Halls, H.C., 1982. The importance of potential of mafic dyke swarms in studies of geodynamic process. Geoscience Canada 9, 129–143.
Halls, H.C., 1987. Dyke swarms and continental rifting some concluding remarks. In: Halls, H.C., Fahrig, W.F. (Eds.), Mafic Dyke Swarms, vol. 34. Geological Association of Canada, pp. 5–24 (special paper).
Halls, H.C., Pesonen, L.J., 1982. Paleomagnetism of Keweenawan rocks. Geological Society of America, Memoir 156, 173–201.
Halls, H.C., Zhang, B., 1995. Tectonic implications of clouded feldspar in Proterozoic mafic dykes. In: Devaraju, T.C. (Ed.), In Dyke Swarms of Peninsular India, vol. 33. Memoir Geological Society of India, pp. 65–80.
Halls, H.C., Kumar, A., Srinivasan, R., Hamilton, M.A., 2007. Paleomagnetism and U–Pb geochronology of easterly trending dykes in the Dharwar craton, India: feldspar clouding, radiating dyke swarms and the position of India at 2.37 Ga. Precambrian Research 155, 47–68.
Hanson, R.E., Gose, W.A., Crowley, J.L., Ramezani, J., Bowring, S.A., Bullen, D.S., Hall, R.P., Pancake, J.A., Mukwakwami, J., 2004a. Paleoproterozoic intraplatemagmatism and basin development on the Kaapvaal Craton: age, paleomagnetism and geochemistry of ~1.93 to ~1 87 Ga post-Waterberg dolerites. South African Journal of Geology 107, 233–254.
Hanson, R.E., Rioux, M., Gose, W.A., Blackburn, T.J., Bowring, S.A., Mukwakwami, J., Jones, D.L., 2011. Paleomagnetic and geochronologicalal evidence for large-scale post–1. 88 Ga displacement between the Zimbabwe and Kaapvaal cratons along the Limpopo belt. Geology 39 (5), 487–490.
Hargraves, R.B., Hattingh, P.J., Onstott, T.C., 1994. Palaeomagnetic results from the Timbavati gabbros in the Kruger National Park, South Africa. South African Journal of Geology 97, 114–118.
Hartmann, L.A., 2002. The mesoproterozoic supercontinent Atlantica in the Brazilian Shield; review of geological and U–Pb zircon and Sm–Nd isotopic evidence. In: Rogers, J.W., Santosh, M. (Eds.), Mesoproterozoic Supercontinent. Gondwana Research 5, 157–163.
Hoffman, P.F., 1988. United plates of America, the birth of a craton. Annual Review of Earth and Planetary Science 16, 543–603.
Hoffman, P.F., 1991. Did the breakout of Laurentia turn Gondwanaland inside out? Science 252, 1409–1412.
Jacobs, J., Pisarevsky, S., Thomas, R.J., Becker, T., 2008. The Kalahari Craton during the assembly and dispersal of Rodinia. Precambrian Research 160, 142–158.
Jayananda, M., Moyen, J.F., Martin, H., Peucat, J.-J., Auvray, B., Mahabalesawar, B., 2000. Late Archaean (2550–2520 Ma) juvenile magmatism in the Eastern

Dharwar craton, southern India: constraints from geochronology, Nd–Sr isotopes and whole rock geochemistry. Precambrian Research 99, 225–254.
Jones, D.L., McElhinny, M.W., 1966. Paleomagnetic correlation of basic intrusions in the Precambrian of southern Africa. Journal of Geophysical Research 71, 543–552.
Jones, D.L., Powell, C.McA., 2001. Palaeomagnetic results from the Umkondo Large Igneous Province and their relevance to Rodinia. In: Fourth International Dyke Conference, South Africa 26–29 June (Program and Abstracts, 34).
Karlstrom, K.E., Harlan, S.S., Williams, M.L., McClelland, J., Geissman, J.W., Ǻ häll, K.I., 1999. Refining Rodinia: geologic evidence for the Australia–western US connection in the Proterozoic. GSA Today 9 (10), 1–7.
Kelly, N.M., Clarke, G.L., Fanning, C.M., 2002. A two-stage evolution of the Neoproterozoic Rayner structural episode: new U–Pb sensitive high resolution ion microprobe constraints from the Oygarden Group, Kemp Land, East Antarctica. Precambrian Research 116, 307–330.
Klootwijk, C.T., Nazirullah, R., de Jong, K.A., 1986. Paleomagnetic constraints on formation of the Mianwali re-entrant, Trans-Indus and Western Salt Range, Pakistan. Earth and Planetary Science Letters 80, 394–414.
Krapez, B., 1999. Stratigraphic record of an Atlantic-type global tectonic cycle in the Palaeoproterozoic Ashburton Province of Western Australia. Australian Journal of Earth Sciences 46, 71–87.
Kumar, B., Das Sharma, S., Sreenivas, B., Dayal, A.M., Rao, M.N., Dubey, N., Chawla, B.R., 2002. Carbon, oxygen and strontium isotope geochemistry of Proterozoic carbonate rocks of the Vindhyan Basin, central India. Precambrian Research 113, 43–63.
Kumar, S., Srivastava, P., 1997. A note on the carbonaceous megafossils from the Neoproterozoic Bhander Group, Maihar area, Madhya Pradesh. Journal of Paleontological Society of India 42, 141–146.
Kumar, S., 2001. Mesoproterozoic megafossil Chuaria–Tawuia association may represent parts of a multicellular plant, Vindhyan Supergroup, central India. Precambrian Research 106, 187–211.
Kumar, A., Bhalla, M.S., 1983. Paleomagnetics and igneous activity of the area adjoining the south-western margin of the Cuddapah basin, India. Geophysical Journal of Royal Astronomical Society 73, 27–37.
Kusky, T.M., Li, J.H., Santosh, M., 2007. The Paleoproterozoic North Hebei Orogen: North China craton's collisional suture with the Columbia supercontinent. Gondwana Research 12, 4–28.
Lauerma, R., 1995. Kursun ja Sallan kartta-alueiden kalliopera. Summary Pre-Quaternary rocks of the Kursu and Salla map-sheet areas. Geological map of Finland 1:100,000, Explanation to the map of Pre-Quaternary Rocks, Sheets 3643, 4621 + 4623, p. 40.
Ledru, P., Johan, V., Milesi, P., Tegyey, M., 1994. Markers of the last stages of the Palaeoproterozoic collision: evidence for a 2 Ga continent involving circum-South Atlantic provinces. Precambrian Research 69, 169–191.
Li, Z.X., Bogdanova, S.V., Collins, A.S., Davidson, A., De Waele, B., Ernst, R.E., Fitzsimons, I.C.W., Fuck, R.A., Gladkochub, D.P., Jacobs, J., Karlstrom, K.E., Lu, S., Natapov, L.M., Pease, V., Pisarevsky, S.A., Thrane, K., Vernikovsky, V., 2008. Assembly, configuration, and break-up history of Rodinia: a synthesis. Precambrian Research 160, 179–210.
Lubnina, N.V., Ernst, R., Klausen, M., Söderlund, U., 2010. Paleomagnetic study of NeoArchean–Paleoproterozoic dykes in the Kaapvaal craton. Precambrian Research 183, 523–552.
Ludwig, K.R., 1999. User's Manual for Isoplot/Ex Version 2.02, A Geochronological Toolkit for Microsoft Excel. Berkeley Geochronology Center Special publication 1a, Berkeley, CA, USA.
Malone, S.J., Meert, J.G., Banerjee, D.M., Pandit, M.K., Tamrat, E., Kamenov, G.D., Pradhan, V.R., Sohl, L.E., 2008. Paleomagnetism and detrital zircon geochronology of the Upper Vindhyan sequence, Son Valley and Rajasthan, India: a ca. 1000 Ma closure age for the Purana basins? Precambrian Research 164, 137–159.
Malviya, V.P., Arima, M., Pati, J.K., Kaneko, Y., 2004. First report of metamorphosed basaltic pillow lava from central part of Bundelkhand craton, India: an Island arc setting of possible Late Archaean age. Gondwana Research 7, 1338–1340.
Malviya, V.P., Arima, M., Pati, J.K., Kaneko, Y., 2006. Petrology and geochemistry of metamorphosed basaltic pillow lava and basaltic komatiite in Mauranipur area: subduction related volcanism in Archean Bundelkhand craton, Central India. Journal of Mineralogical and Petrological Sciences 101, 199–217.
Mazumdar, R., Banerjee, D.M., 2001. Regional variations in the carbon isotopic composition of phosphorite fromthe Early Cambrian Lower Tal formation, Mussoorie Hills, India. Chemical Geology 175, 5–15.
McElhinny, M.W., Cowley, J.A., Edwards, D.J., 1978. Palaeomagnetism of some rocks from peninsular India and Kashmir. Tectonophysics 50, 41–54.
McMenamin, M.A.S., McMenamin, D.L.S., 1990. The Emergence of Animals: the Cambrian Breakthrough. Columbia University Press, New York, p. 217.
Meert, J.G., 2001. Growing Gondwana and rethinking Rodinia. Gondwana Research 4, 279–288.
Meert, J.G., 2002. Paleomagnetic evidence for a Paleo–Mesoproterozoic supercontinent Columbia. Gondwana Research 5, 207–216.
Meert, J.G., 2003. A synopsis of events related to the assembly of eastern Gondwana. Tectonophysics 362, 1–40.
Meert, J.G., 2009. In GAD we trust. Nature Geosciences News and Views 2, 673–674.
Meert, J.G., Pandit, M.K., Pradhan, V.R., Banks, J.C., Sirianni, R., Stroud, M., Newstead, B., Gifford, J., 2010. The Precambrian tectonic evolution of India: A 3.0 billion year odyssey. Journal of Asian Earth Sciences 39, 483–515.
Meert, J.G., Pandit, M.K., Pradhan, V.R., 2011. Preliminary report on the paleomagnetism of 1.88 Ga dykes from the Bastar and Dharwar cratons, Peninsular India. Gondwana Research, doi:10.1016/j.gr.2011.03.005.
Meert, J.G., Van der Voo, R., Ayub, S., 1995. Paleomagnetic investigation of the Gagwe lavas and Mbozi Complex, Tanzania and the assembly of Gondwana. Precambrian Research 74, 225–244.
Meert, J.G., Van der Voo, R., 1996. Paleomagnetic and $^{40}Ar/^{39}Ar$ study of the Sinyai dolerite, Kenya: implications for Gondwana assembly. Journal of Geology 104, 131–142.
Meert, J.G., Powell, C. McA., 2001. Assembly and breakup of Rodinia. Precambrian Research 110, 1–8.
Meert, J.G., Stuckey, W., 2002. Revisiting the paleomagnetism of the 1.476 Ga St. Francois Mountains igneous province. Missouri Tectonics 21 (2), 19.
Meert, J.G., Torsvik, T.H., 2003. The making and unmaking of a supercontinent: Rodinia revisted. Tectonophysics 375, 261–288.
Mertanen, S., Pesonen, L.J., 1994. Preliminary results of the palaeomagnetic and rock magnetic study of the early Proterozoic Tsuomasvarri ultramafic and gabbrodiorite intrusion, northern Fennoscandia. Precambrian Research 69, 25–50.
Mertanen, S., Pesonen, L.J., Huhma, H., 1996. Palaeomagnetism and Sm–Nd ages of the Neoproterozoic diabase dykes in Laanila and Kautokeino, northern Fennoscandia. In: Brewer, T.S. (Ed.), Precambrian Crustal Evolution in the North Atlantic Region. Geological Society of London, Special Publication 112, 331–358.
Miller, K.C., Hargraves, R.B., 1994. Paleomagnetism of some Indian kimberlites and lamproites. Precambrian Research 69, 259–267.
Mondal, M.E.A., Zainuddin, S.M., 1996. Evolution of Archean–Palaeoproterozoic Bundelkhand massif, Central India—evidence from granitoid geochemistry. Terra Nova 8, 532–539.
Mondal, M.E.A., Deomurari, M.P., Goswami, J.N., Rahman, A., Sharma, K.K., 1997. $^{207}Pb/^{206}Pb$ zircon ages of samples from Bundelkhand massif, Central India. In: Abstract in International Conference on Isotopes in Solar System, pp. 80–81.
Mondal, M.E.A., Sharma, K.K., Rahman, A., Goswami, J.N., 1998. Ion microprobe $^{207}Pb/^{206}Pb$ zircon ages for gneiss–granitoid rocks from Bundelkhand massif: evidence for Archean components. Current Science 74, 70–75.
Mondal, M.E.A., Goswami, J.N., Deomurari, M.P., Sharma, K.K., 2002. Ion microprobe $^{207}Pb/^{206}Pb$ ages of zircons from the Bundelkhand Massif, northern India: implications for crustal evolution of the Bundelkhand–Aravalli supercontinent. Precambrian Research 117, 85–100.
Moores, E.M., 1991. Southwest U.S.–East Antarctic (SWEAT) connection: a hypothesis. Geology 19, 425–428.
Mueller, P.A., Kamenov, G.D., Heatherington, A.L., Richards, J., 2008. Crustal evolution in the Southern Appalachian Orogen; evidence from Hf isotopes in detrital zircons. Journal of Geology 116, 414–422.
Murthy, N.G.K., 1995. Proterozoicmaficdykes in southern peninsular India: a review. In: Devaraju, T.C. (Ed.), Mafic Dyke Swarms of Peninsular India, vol. 33. Geological Society of India, Memoir, pp. 81–98.
Murthy, Y.G.K., Babu Rao, V., Guptasarma, D., Rao, J.M., Rao, M.N., Bhattacharji, S., 1987. Tectonic, petrochemical and geophysical studies of mafic dyke swarms around the Proterozoic Cuddapah Basin south India. In: Halls, H.C., Fahrig, W. (Eds.), Mafic Dyke Swarms, vol. 34. Geology Association of Canada Special Paper, pp. 303–316.
Naqvi, S.M., Rogers, J.J.W., 1987. Precambrian Geology of India. Oxford University Press Inc, p. 223.
Neuvonen, K.J., Pesonen, L.J., Pietarinen, H., 1997. Remanent magnetization in the Archaean basement and cutting dykes in Finland, Fennoscandian shield. In: Pesonen, L.J. (Ed.), The Lithosphere of Finland—a Special Issue of the Finnish Lithosphere Programme. Geophysica 33, 111–146.
Nomade, S., Chen, Y., Feraud, G., Pouclet, A., Theveniaut, H., 2001. First paleomagnetic and $^{40}Ar/^{39}Ar$ study of Paleoproterozoic rocks from the French Guyna (Camopi and Oypok rivers), northeastern Guyana Shield. Precambrian Research 109, 230–256.
Nomade, S., Chen, Y., Pouclet, A., Fïeraud, G., Thĭeveniaut, H., Daouda, B.Y., Vidal, M., Rigolet, C., 2003. The Guiana and the West African Shield Palaeoproterozoic grouping: new palaeomagnetic data for French Guiana and the Ivory Coast. Geophysical Journal International 154, 677–694.
Oldham, R.D., 1893. A manual of the Geology of India, 2nd edition. Govt. of India, Publication, Calcutta.
Onstott, T.C., Hargraves, R.B., 1981. Proterozoic transcurrent tectonics: palaeomagnetic evidence from Venezuela and Africa. Nature 289, 131–136.
Onstott, T.C., Dorbor, J., 1987. $^{40}Ar/^{39}Ar$ and paleomagnetic results from Liberia and the Precambrian APW database for the West African Shield. Journal of African Earth Sciences 6, 537–552.
Park, J.K., Buchan, K.L., Harlan, S.S., 1995. A proposed giant radiating dyke swarm fragmented by the separation of Laurentia and Australia based on paleomagnetism of ca. 780 Ma mafic intrusions in western North America. Earth and Planetary Science Letters 132, 129–139.
Patchett, P.J., Bylund, G., 1977. Age of Grenville Belt magnetization: Rb–Sr and paleomagnetic evidence from Swedish dolerites. Earth and Planetary Science Letters 35, 92–104.
Pati, J.K., Raju, S., Mamgain, V.D., Shankar, R., 1997. Record of gold mineralization in parts of Bundelkhand Granitoid Complex (BGC). Journal of Geological Society of India 50, 601–606.
Pati, J.K., 1999. Study of granitoid mylonites and reef/vein quartz in parts of Bundelkhand Granitoid Complex (BGC). Records Geological Survey of India 131 (8), 95–96.
Pati, J.K., Patel, S.C., Pruseth, K.L., Malviya, V.P., Arima, M., Raju, S., Pati, P., Prakash, K., 2007. Geochemistry of giant quartz veins from the Bundelkhand craton, Central India and its implications. Journal of Earth System Science 116, 510–697.

Pati, J.K., Raju, S., Malviya, V.P., Bhushan, R., Prakash, K., Patel, S.C., 2008. Mafic dykes of Bundelkhand craton, Central India: field, petrological and geochemical characteristics. In: Srivastava, R., et al. (Eds.), Indian Dykes: Geochemistry, Geophysics and Geochronology. Narosa Publishing House, New Delhi, pp. 547–569.
Paul, D.K., Potts, P.J., Gibson, I.L., Harris, P.G., 1975. Rare-earth abundances in Indian kimberlites. Earth and Planetary Science Letters 25, 151–158.
Payne, J.L., Hand, M., Barovich, K.M., Reid, A., Evans, D.A.D., 2009. Correlations and reconstruction models for the 2500–1500 Ma evolution of the Mawson continent. Geological Society of London, Special Publication 323, 319–355.
Pesonen, L.J., Neuvonen, K.J., 1981. Paleomagnetism of the Baltic shield – implications for Precambrian tectonics. In: Kröner, A. (Ed.), Precambrian Plate Tectonics. Elsevier, Amsterdam, pp. 623–648.
Pesonen, L.J., Reimold, W.U., Gibson, R.L., 2002. Preliminary paleomagnetic and rock magnetic data of the Vredefort structure, South Africa. In: Abstracts of the 33rd LPSC, Houston, March 4–8, 2002 (CD-ROM).
Pesonen, L.J., Elming, S.A., Mertanen, S., Pisarevsky, S., D'Agrella, M.S., Meert, J.G., Schmidt, P.W., Abrahamsen, N., Bylund, G., 2003. Palaeomagnetic configuration of continents during the Proterozoic. Tectonophysics 375, 289–324.
Piispa, E.J., Smirnov, A.V., Pesonen, L.J., Lingadevaru, M., Ananthar-Murthy, K.J., Devaraju, T.C., 2011. An integrated study of Proterozoic dykes, Dharwar craton southern India. In: Srivastava, R.K. (Ed.), Dyke Swarms: Keys for Geodynamic Interpretation. Springer-Verlag, Heidelberg, pp. 33–45.
Pisarevsky, S.A., Sokolov, S.J., 1999. Palaeomagnetism of the Palaeoproterozoic ultramafic intrusion near Lake Konchozero, Southern Karelia, Russia. Precambrian Research 93, 201–213.
Pisarevsky, S.A., Natapov, L.M., 2003. Siberia and Rodinia. Tectonophysics 375, 221–245.
Pisarevsky, S.A., Murphy, J.B., Cawood, P.A., Collins, A.S., 2008. Late Neoproterozoic and Early Cambrian Paleogeography: Models and Problems. Geological Society of London 294, 9–31.
Poitou, C., Kumar, A., Valet, J., Mamila, V., Besse, J., Rao, M., Rao, P., 2008. Paleomagnetism of the Bundelkhand Dyke swarms, Madhya Pradesh, Central India. In: Abstract, AGU, Fall Meeting.
Poorter, R.P.E., 1975. Palaeomagnetism of Precambrian rocks from southeast Norway and south Sweden. Physical Earth and Planetary International 10, 74–87.
Powell, C. McA., Jones, D.L., Pisarevsky, S.A., Wingate, M.T.D., 2001. Paleomagnetic constraints on the position of the Kalahari craton in Rodinia. Precambrian Research 110, 33–46.
Powell, C. McA., Pisarevsky, S.A., 2002. Late Neoproterozoic assembly of east Gondwana. Geology 3, 3–6.
Pradhan, V.R., Pandit, M.K., Meert, J.G., 2008. A cautionary note on the age of the Paleomagnetic pole obtained from the Harohalli Dyke swarms, Dharwar Craton, Southern India. In: Srivastava, et al. (Eds.), Indian Dykes: Geochemistry, Geophysics and Geochronology. Narosa Publishing House, India, pp. 339–351.
Pradhan, V.R., Meert, J.G., Pandit, M.K., Kamenov, G., Gregory, L.C., Malone, S., 2010. India's changing place in global Proterozoic reconstructions: new geochronologic constraints on key paleomagnetic poles from the Dharwar and Aravalli/Bundelkhand Cratons. Journal of Geodynamics 50, 224–242.
Radhakrishna, T., Piper, J.D.A. (eds), 1999. The Indian Subcontinent and Gondwana: a Palaeomagnetic and Rock Magnetic Perspective. Geological Society of India Memoir 44, pp 270.
Rai, V., Shukla, M., Gautam Vibhuti, R., 1997. Discovery of carbonaceous megafossils (Chuaria–Tawuia assemblage) fromtheNeoproterozoic Vindhyan succession (Rewa Group), Allahabad, India. Current Science 73, 783–788.
Rainbird, R.H., Stern, R.A., Khudoley, A.K., Kropachev, A.P., Heaman, L.M., Sukhorukov, V.I., 1998. U–Pb geochronology of Riphean sandstone and gabbro from Southeast Siberia and its bearing on the Laurentia–Siberia connection. Earth and Planetary Science Letters 164, 409–420.
Ramchandra, H.M., Mishra, V.P., Deshmukh, S.S., 1995. Mafic dykes in the Bastar Precambrian: study of the Bhanupratappur–Keskal mafic dyke swarm. In: Devaraju, T.C. (Ed.), Mafic Dyke Swarms of Peninsular India, vol. 33. Memoirs Geological Society of India, pp. 183–207.
Rao, J.M., Rao, G.V.S.P., Widdowson, M., Kelley, S.P., 2005. Evolution of Proterozoic mafic dyke swarms of the Bundelkhand Granite Massif, Central India. Current Science 88, 502–506.
Rao, J.M., 2004. The wide-spread 2 Ga dyke activity in the Indian shield—evidences from Bundelkhand mafic dyke swarm, Central India and their tectonic implications. Gondwana Research 7, 1219–1228.
Rasmussen, B., Bose, P.K., Sakar, S., Banerjee, S., Fletcher, I.R., McNaughton, N.J., 2002a. 1.6 Ga U–Pb zircon age for the Chorhat Sandstone, lower Vindhyan, India: possible implications for the early evolution of animals. Geology 20, 103–106.
Rasmussen, B., Fletcher, I.R., Bengtson, S., McNaughton, N.J., 2002b. Discoidal impressions and trace-like fossils more than 1200 million years old. Science 296, 1112–1115.
Ratre, K., Waele, B.D., Biswal, T.K., Sinha, S., 2010. SHRIMP geochronology for the 1450 Ma Lakhna dyke swarm: its implication for the presence of Eoarchean crust in the Bastar craton and 1450–570 Ma depositional age for Purana basin (Khariar) Eastern Indian Peninsula. Journal of Asian Earth Sciences 39, 563–577.
Ray, J.S., Martin, M.W., Veizer, J., Bowring, S.A., 2002. U–Pb Zircon dating and Sr isotope systematic of the Vindhyan SuperGroup, India. Geology 30, 131–134.
Ray, J.S., Veizer, J., Davis, W.J., 2003. C, O, Sr and Pb isotope systematics of carbonate sequences of the Vindhyan SuperGroup India: age, diagenesis, correlations, and implications for global events. Precambrian Research 121, 103–140.
Renne, P.R., Onstott, T.C., D'Agrella-Filho, M.S., Pacca, I.G., Teixeira, W., 1990. $^{40}Ar/^{39}Ar$ dating of 1 0–1. 1 Ga magnetizations from the São Francisco and Kaapvaal Cratons: tectonic implications for Pan-African and Brasiliano mobile belts. Earth and Planetary Science Letters 101, 349–366.
Rogers, J.J.W., 1996. A history of the continents in the past three billion years. Journal of Geology 104, 91–107.
Rogers, J.J.W., Santosh, M., 2002. Configuration of Columbia, a Mesoproterozoic supercontinent. Gondwana Research 5, 5–22.
Rogers, J.J.W., Santosh, M., 2003. Supercontinent in earth history. Gondwana Research 6, 417–434.
Roy, A.B., Paliwal, B.S., Shekhawat, S.S., Nagori, D.K., Golani, P.R., Bejarniya, B.R., 1988. In: Roy, A.B. (Ed.), Stratigraphy of the Aravalli Supergroup in the type area; in Precambrian of the Aravalli Mountain, Rajasthan India, vol. 7. Geological Society of India, Memoir, pp. 121–138.
Roy, A.B., Kröner, A., 1996. Single zircon evaporation ages constraining the growth of the Archean Aravalli craton, northwestern Indian shield. Geology Magazine 133, 333–342.
Salminen, J., Pesonen, L.J., Reimold, W.U., Donadini, F., Gibson, R.L., 2009. Paleomagnetic and rock magnetic study of the Vredefort impact structure and the Johannesburg Dome, Kaapvaal Craton South Africa – implications for the apparent polar wander path of the Kaapvaal Craton during the Mesoproterozoic. Precambrian Research 168, 167–184.
Santosh, M., Yokoyama, K., Biju-Shekhar, S., Rogers, J.J.W., 2003. Multiple tectonothermal events in the granulite blocks of southern India revealed from EPMA dating: implications on the history of supercontinents. Gondwana Research 6, 29–63.
Sarangi, S., Gopalan, K., Kumar, S., 2004. Pb–Pb age of earliestmegascopic, eukaryotic alga bearing Rhotas formation Vindhyan SuperGroup, India: implications for Precambrian atmospheric oxygen evolution. Precambrian Research 121, 107–121.
Sarkar, A., Paul, D.K., Potts, P.J., 1996. Geochronology and geochemistry of Mid-Archaean trondhjemitic gneisses from the Bundelkhand craton, central India. Records Research in Geology and Geophysics of Precambrians 16, 76–92.
Sarkar, A., Ghosh, S., Singhai, R.K., Gupta, S.N., 1997. Rb–Sr geochronology of the Dargawan sill: constraint on the age of the type Bijawar sequence of Central India. In: International Conf. on isotopes in Solar System, November 11–14, vol. 5, pp. 100–101.
Sarkar, G., Corfu, F., Paul, D.K., McNaughton, N.J., Gupta, S.N., Bishui, P.K., 1993. Early Archean crust in Bastar craton Central India – a geochemical and isotopic study. Precambrian Research 62, 127–137.
Sears, J.W., Price, R.A., 2000. New look at the Siberian connection: no SWEAT. Geology 28, 423–426.
Sears, J.W., Price, R.A., 2003. Tightening the Siberian connection to western Laurentia. GSA Bulletin 115, 943–953.
Sharma, K.K., 1998. Geological evolution and crustal growth of Bundelkhand craton and its relict in the surrounding regions, North Indian Shield. In: Paliwal, B.S. (Ed.), The Indian Precambrian. Scientific Publishers, Jodhpur, pp. 33–43.
Sharma, K.K., Rahman, A., 1996. Mafic dykes in Bundelkhand granitoids and mafic volcanics in Supra-batholithic volcanosedimentaries (Bijawar). DST Newsletters 15, 17–19.
Sharma, K.K., Rahman, A., 2000. The early Archaean–Paleoproterozoic crustal growth of the Bundelkhand craton northern Indian shield. In: Deb, M. (Ed.), Crustal Evolution and Metallogeny in the Northwestern Indian Shield. Narosa Publishing House, New Delhi, pp. 51–72.
Sinha Roy, S., Malhotra, G., Mohanty, M., 1998. Geology of Rajasthan. Geological Society of India, Bangalore, p. 278.
Smith, C.B., 1992. The Age of the Majhgawan Pipe, India. Scott Smith Petrology 9.
Söderlund, U., Hofmann, A., Klausen, M.B., Olsson, J.R., Ernst, R.C., Persson, P., 2010. Towards a complete magmatic barcode for the Zimbabwe craton: Baddeleyite U–Pb dating of regional dolerite dyke swarms and sill complexes. Precambrian Research 183, 388–398.
Srivastava, A.P., Rajagopalan, G., 1988. F–T Ages of the Vindhyan Glauconitic sandstone beds exposed around the Rawatbhata area, Rajasthan. Journal of Geological Society of India 32, 527–529.
Srivastava, R.K., Chalapathi, S., Chalapthi, R.N.V., 2008. Dyke swarms of Indian shield in space and time. In: Indian Dykes: Geochemistry, Geophysics and Geochronology. Narosa Publishing Ltd., New Delhi, India, p. 650.
Srivastava, R.K., Gautam, G.C., 2008. Precambrian mafic dyke swarms from the southern Bastar Central India craton: present and future perspectives. In: Srivastava, R.K., Sivaji, Ch., Chalapati Rao, N.V. (Eds.), Indian Dykes: Geochemistry, Geophysics, and Geochronology. Narosa Publishing Ltd., New Delhi, India, pp. 367–376.
Stearn, J.E.F., Piper, J.D.A., 1984. Palaeomagnetism of the Sveconorwegian mobile belt of the Fennoscandian Shield. Precambrian Research 23, 201–246.
Stein, H.J., Hannah, J.L., Zimmerman, A., Markey, R.J., Sarkar, S.C., Pal, A.B., 2004. A 2.5 Ga porphyry Cu–Mo–Au deposit at Malanjhkhand, central India; implications for late Archean continental assembly. Precambrian Research 134, 189–226.
Swanson-Hysell, N.L., Maloof, A.C., Weiss, B.P., Evans, D.A.D., 2009. Nature Geosciences 2, 713–717.
Torsvik, T.H., Briden, J.C., Smethurst, M.A., 2000. IAPD 2000. Norwegian Geophysical Union.
Torsvik, T.H., Carter, L.M., Ashwal, L.D., Bhushan, S.K., Pandit, M.K., Jamtveit, B., 2001. Rodinia refined or obscured: palaeomagnetism of the Malani Igneous Suite (NW India). Precambrian Research 108, 319–333.

Van der Voo, R., 1990. The reliability of paleomagnetic data. Tectonophysics 184, 1–9.
Van der Voo, R., Meert, J.G., 1991. Late Proterozoic paleomagnetism and tectonic models: a critical appraisal. Precambrian Research 53, 149–163.
Venkatachala, B.S., Mukund, S., Shukla, M., 1996. Age and Life of the Vindhyans – facts and conjectures. Memoir Geological Society of India 36, 137–155.
Vinogradov, A.P., Tugarinov, A.I., Zhikov, C.I., Stanikova, N.I., Bibikova, E.V., Khorre, K., 1964. Geochronology of the Indian Precambrian. In: Report of the 22nd International Congress, New Delhi, pp. 553–567 (10).
Wang, Y., Liu, D., Chung, S.L., Tong, L., Ren, L., 2008. SHRIMP zircon age constraints from the Larsemann Hills region Prydz Bay, for a late Mesoproterozoic to early Neoproterozoic tectono-thermal event in East Antarctica. American Journal of Science 308, 573–617.
Wiedenbeck, M., Goswami, J.N., 1994. High precision $^{207}Pb/^{206}Pb$ zircon geochronology using a small ion probe. Geochimica Cosmochimica Acta 58, 2135–2141.
Wiedenbeck, M., Goswami, J.N., Roy, A.B., 1996. Stabilization of the Aravalli Craton of northwestern India at 2.5 Ga: an ion microprobe zircon study. Chemical Geology 129, 325–340.
Weil, A.B., Van der Voo, R., MacNiocall, C., Meert, J.G., 1998. The Proterozoic supercontinent Rodinia: paleomagnetically derived reconstructions for 1100–800 Ma. Earth and Planetary Science Letters 154, 13–24.
Wingate, M.T.D, Pisarevsky, S.A., Evans, D.A.D., 2002. Rodinia connection between Australia and Laurentia; no SWEAT, no AUSWUS? Terra Nova 14, 121–128.
Young, G.M., 1995. Are Neoproterozoic glacial deposits preserved on the margins of Laurentia related to the fragmentation of two supercontinents? Geology 23, 153–156.
Zhang, S.H., Li, Z.X., Wu, H.C., 2006. New Precambrian palaeomagnetic constraints on the position of the North China Block in Rodinia. Precambrian Research 144, 213–238.
Zhao, G.C., Cawood, P.A., Wilde, S.A., Sun, M., 2002. Review of global 2.1–1.8 Ga orogens: implications for a pre-Rodinia supercontinent. Earth Science Reviews 59, 125–162.
Zhao, G.C., Sun, M., Wilde, S.A., Li, S.Z., 2004a. A Paleo–Mesoproterozoic supercontinent: assembly, growth and breakup. Earth Science Reviews 67, 91–123.
Zhao, T.P., Zhai, M.G., Xia, B., Li, H.M., Zhang, Y.X., Wan, Y.S., 2004b. Zircon U–Pb SHRIMP dating for the volcanic rocks of the Xiong'er Group: constraints on the initial formation age of the cover of the North China Craton. Chinese Science Bulletin 49, 2495–2502.